FLUCTUATIONS OF SPACE-CHARGE-LIMITED

CURRENTS IN GERMANIUM

by

DAVID JOHN HUNTLEY

B.A.Sc., University of British Columbia, 1957

A THESIS SUBMITTED IN PARTIAL FULFILMENT OF

THE REQUIREMENTS FOR THE DEGREE OF

MASTER OF APPLIED SCIENCE

in the Department

of

Physics

We accept this thesis as conforming to the

required standard

THE UNIVERSITY OF BRITISH COLUMBIA

August 1959

Abstract

The d-c. and a-c. characteristics of p-n-p diodes were measured and interpreted on the basis of present theories. The equivalent parallel capacitance of these diodes was found to decrease as $f^{-\frac{3}{2}}$ at high frequencies in accordance with diffusion theory; from these measurements the lifetime of a hole in the base was estimated to be about 10 microseconds.

The current fluctuations in the diode were measured by comparing them with a standard noise diode, and the results represented as a shunt noise current generator. From the frequency spectrum of the noise it was deduced that it consisted mainly of excess or 1/f noise except at low currents and high frequencies, and here the results were interpreted as a combination of shot and thermal noise. The deduced hot carrier temperature was compared with the theoretical values of Shockley and poor agreement was obtained, indicating inadequacy of the present theory.

Contents

Contents   (continued)

Figures

Figures   (continued)

Acknowledgements

I would like to express my thanks to Professor R.E.Burgess who has shown a great deal of interest in the work and who provided the necessary guidance.

I also wish to thank the National Research Council of Canada for financial support in the form of a Studentship and Summer Supplement.

Chapter I -- INTRODUCTION

1.1   Object and Scope of Thesis

The object of this work is to observe and measure
fluctuations in space-charge-limited currents in germanium
and to interpret these in terms of shot and thermal noise
components. From this it is possible to determine the
effective temperature of carriers in germanium at moderate
electric fields and to compare these temperatures with those
predicted by Shockley (1951).

The effective temperature is calculated from measurements
of the noise in the current flowing through a p-n-p trans-
istor connected as a diode with the base floating, and from
impedance measurements of the same diode. To be able to
correlate carrier temperatures with the noise measured, it is
necessary to have a model of the transistor which is in accord
with both the d-c. and a-c. characteristics and in which we
can place noise current generators to correspnd to drift and
thermal motion of the carriers.

1.2   Physical Structure of a p-n-p Transistor

The cross section of a typical p-n-p transistor is shown
in figure 1. The base is made of low impurity, high resistivity
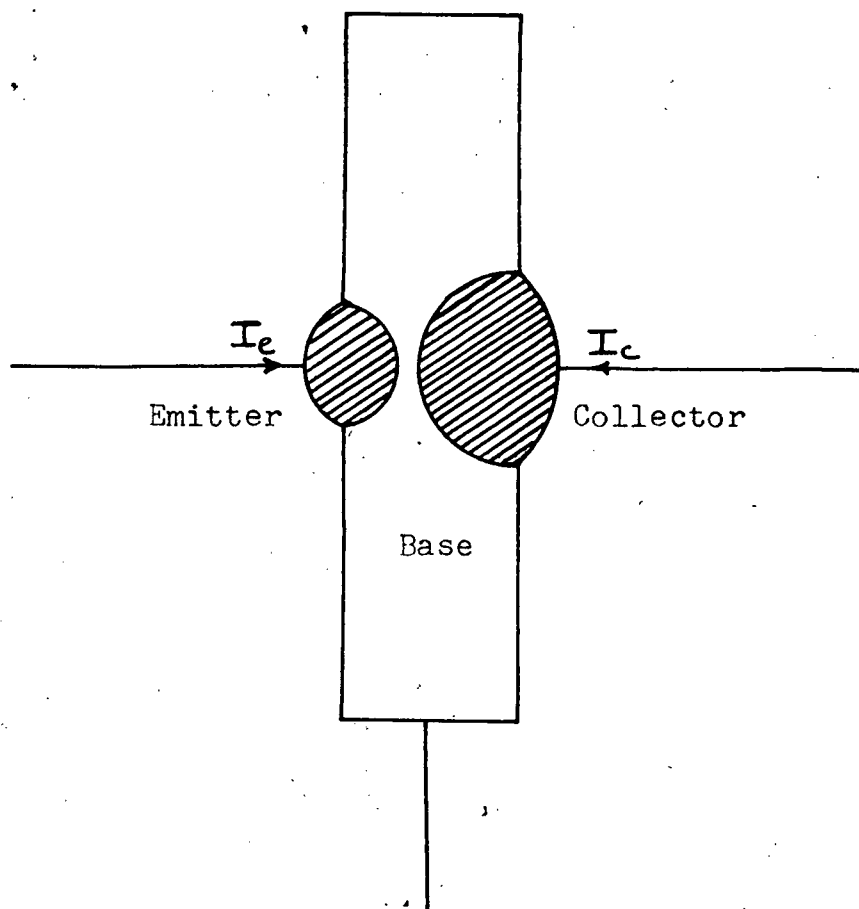
Figure 1 - The Physical Structure of a P-n-p Transistor

material while the emitter and collector are made of high
impurity, low resistivity material; thus if a voltage is
applied between the emitter and collector terminals most of
it will appear across the p-n junction space-charge layers
in the base.

Shockley (1949) has derived the formula for the current
flowing across a single p-n junction,

$$I = I_s \left[\exp\left(\frac{qV_0}{kT}\right) - 1 \right] \qquad (1.2.1)$$

where q = the electronic charge,
         k = Boltzmann's constant,
         T = the absolute temperature of the junction,
         V_0 = the voltage across the junction, positive for
forward bias, and
         I_s = the saturation current under reverse bias.

This formula is derived from the consideration of the diffusion
currents of holes and electrons; if the p region is much more
heavily doped than the n region, only the hole current will
be significant. The reverse saturation current in this case
is given by

$$I_s = \frac{q\, P_n D_P A}{L_P} \qquad (1.2.2)$$

where P_n = the normal hole concentration in the n region,
         D_P = the hole diffusivity in the n region,
         L_P = the diffusion length for holes in the n region, and
         A = the area of the junction.

It must be noted that equation (1.2.1) holds only when the
minority carrier concentrations far from the junction have
their normal values. In a p-n-p transistor the latter condition
is not fulfilled in the n region since the hole diffusion length
in the base is much greater than the base width and therefore

Neutral
Region

Space-charge Region

⊕ Donor Ions

— Free Electrons
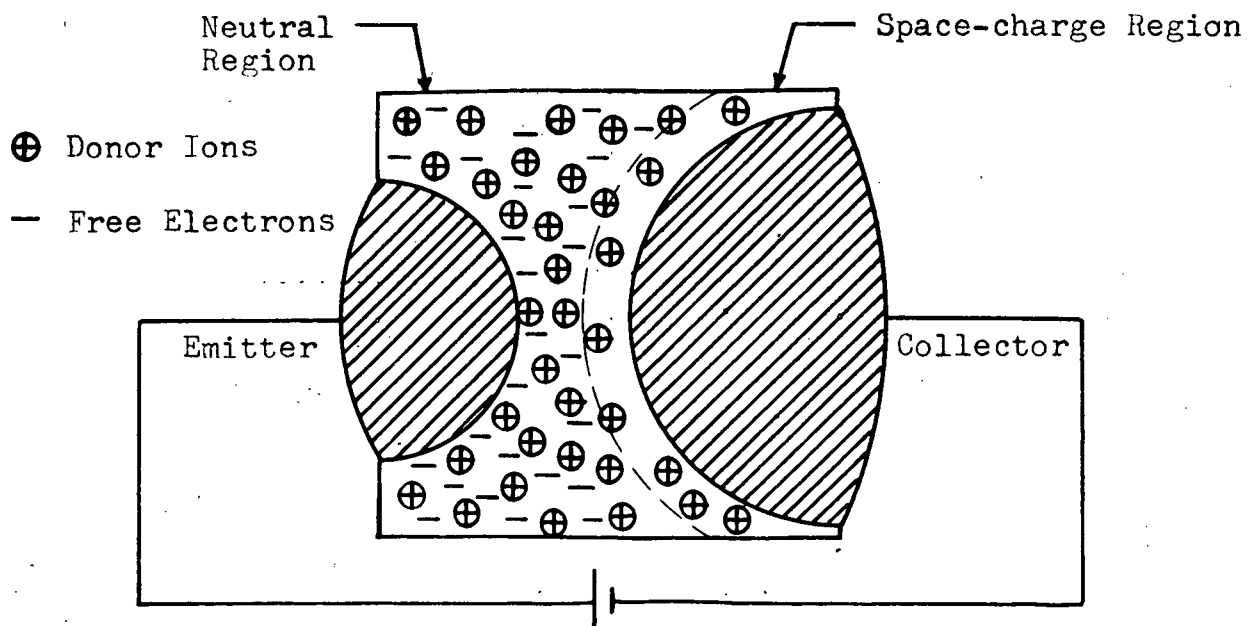
Emitter

Collector

Figure 2a - A P-n-p Diode with Voltage less than V_p.

Neutral
Region

Space-charge Region
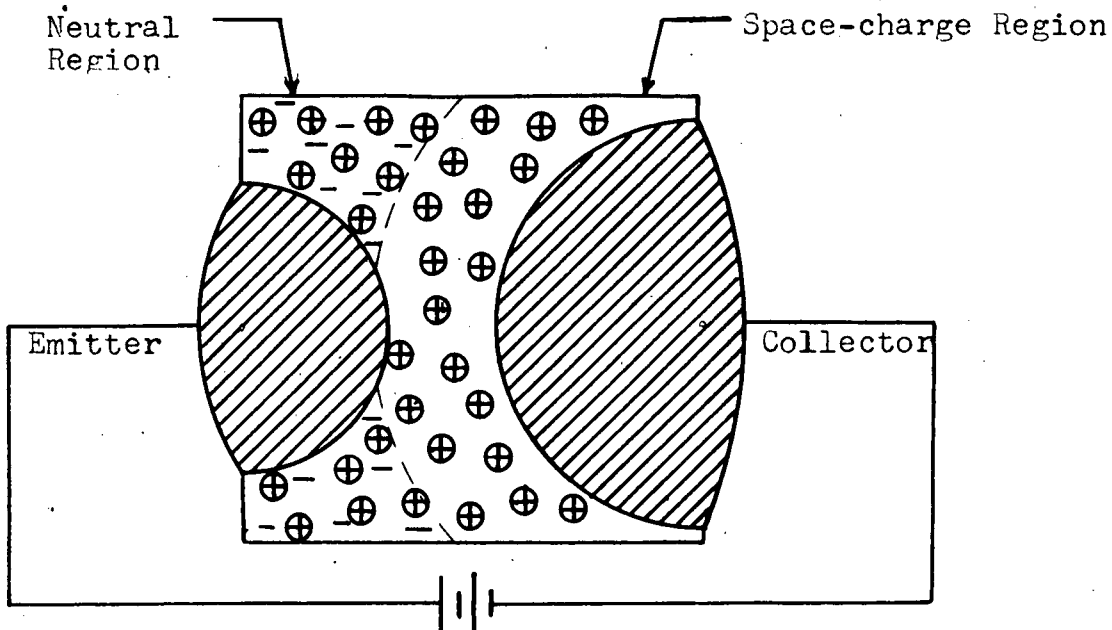
Emitter

Collector

Figure 2b - A P-n-p Transistor with Voltage Greater than V_p.

the two junctions strongly interact (see Appendix I). The
current that flows in an emitter-collector diode for small
voltages has been investigated by Götzberger (1959) who
considers the variation of effective base width with voltage
and also the effects of non-planar geometry of the base. These
are discussed more fully in chapter II. As the voltage across
such a diode is increased, there is a steady increase of
current and at a certain voltage there is a very rapid increase
of current; this occurs when the effective base width becomes
zero, the corresponding voltage being the punch-through voltage.

1.3 . The Punch-through Phenomenon

If an external voltage is applied between the emitter and
collector of a transistor with the base floating, space-charge
layers will form in front of both junctions. In the case of
a p-n-p transistor, the free electrons in the base are repelled
by the negative collector voltage and a space-charge layer of
positive donor ions forms in front of the collector junction.
That voltage at which this layer just touches the emitter is
called the punch-through voltage V_p , and is characterized by
an increase in current due to the injection of holes from the
emitter. Figures 2a and 2b show a transistor with voltages
with less than and slightly greater than V_p respectively, and
figure 3 shows the potential distribution in the base for
various applied voltages.

The punch-through phenomenon is much more vividly seen
by observing the floating emitter potential when a bias is
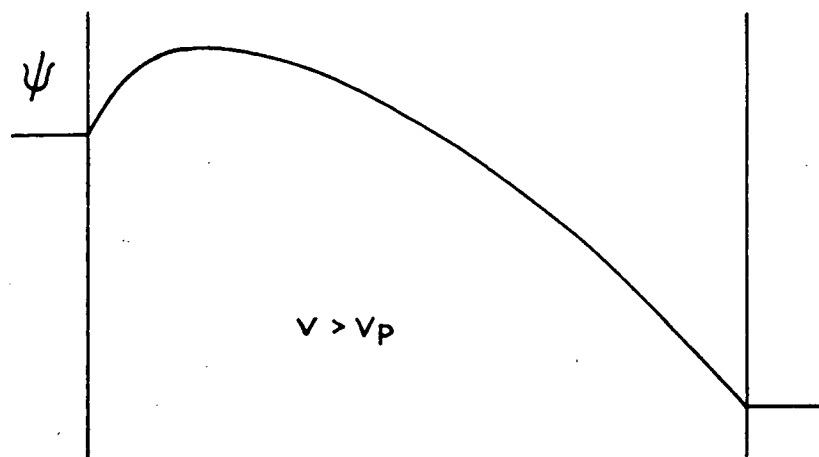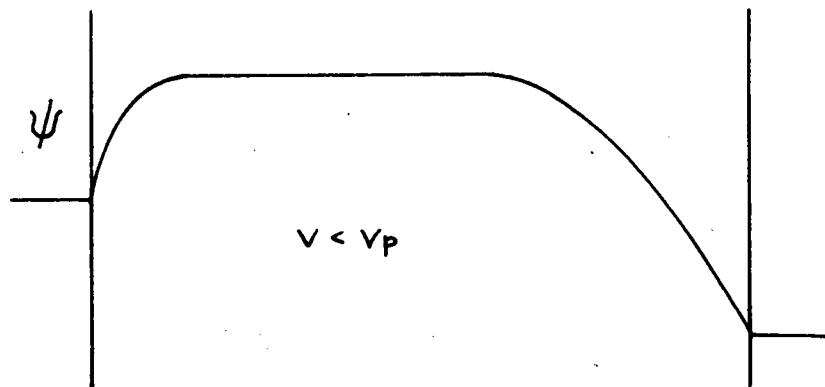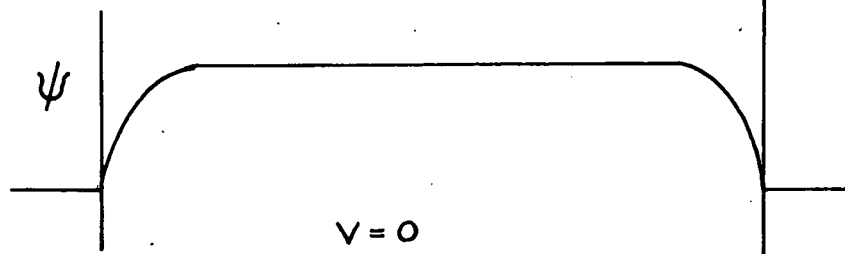
Figure 3 - Potential in the Base under Various Applied Voltages

applied between the collector and base. Up to punch-through the

emitter assumes a potential approximately 0.1 volt below that

of the base, due to the siphon effect discussed in section 1.4.

At the punch-through voltage the floating emitter becomes

completely locked to the collector with a voltage difference

of V_p . This is observed without deviation until breakdown

occurs and for a p-n-p transistor for $V_p \leqslant -V_{cb} \leqslant V_B$, $+V_{eb} = +V_{cb} + V_p$

where V_{cb} and V_{eb} are the collector and emitter voltages

measured with respect to the base, and V_B is the collector-base

breakdown voltage; V_p and V_B are both always considered to be

positive quantities. The value of V_p obtained by this method

may be called the Schenkel-Statz punch-through voltage since

it can be very easily determined using the circuit devised

by them (1954) shown in figure 4a; a typical oscilloscope

trace is shown in figure 4b.

The value of V_p can be predicted theoretically from a

knowledge of the base width and base impurity concentration;

the integration in one dimension of Poisson's equation across

the base yields for a uniform impurity density

$$V_P = \frac{qN}{2\epsilon} W^2 \qquad (1.3.1)$$

where N = the donor ion density in the base,
   ϵ = the permittivity of the base material, and
   W = the base width.

Punch-through can be observed equally well by biasing the

emitter and observing the floating collector potential; exactly

the same value of V_p is obtained provided that the impurity

density is uniform throughout the base, however, if it is not

uniform, in general a different value of V_p will be obtained.

Variable
a-c.
Voltage
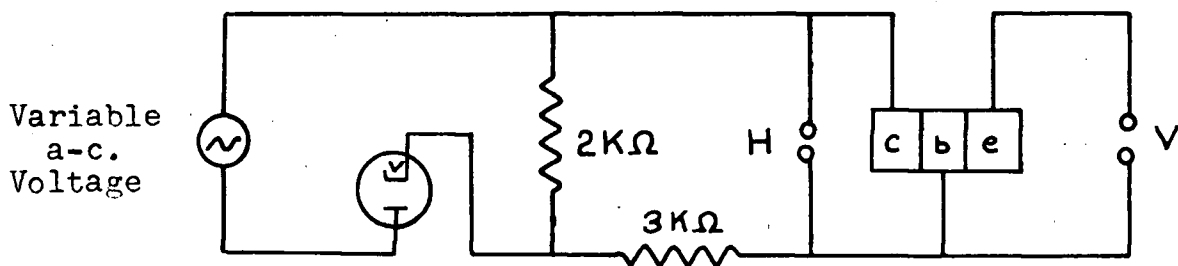
H to Horizontal Sweep of Oscilloscope
V to Vertical Sweep of Oscilloscope

Figure 4a - Schenkel-Statz Circuit for Measuring the Punch-
              Through Voltage of a P-n-p Transistor
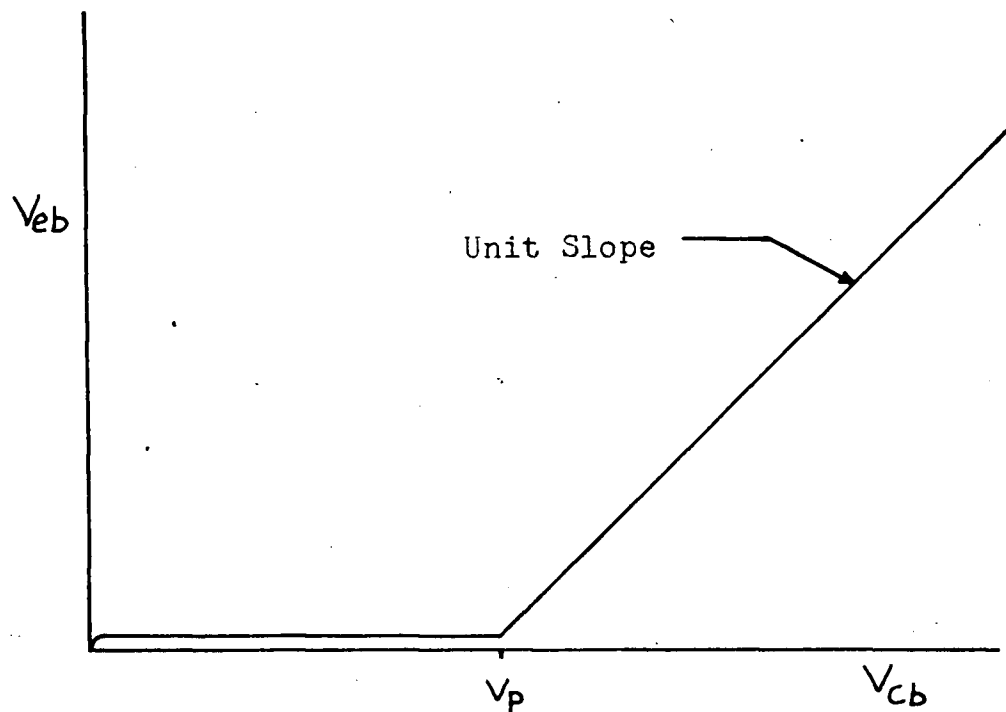
Figure 4b - Typical Oscilloscope Trace Obtained during a
              Schenkel-Statz Test.

In addition, the oscilloscope trace of figure 4b will be rounded at V_p if the emitter junction is diffused into the base such as in grown junction transistors.

The current-voltage characteristics of an emitter-collector diode biased past punch-through have been studied by Nichol (1958); the basic result obtained is that $I \propto (V-V_p)^3$ where V is the emitter voltage measured with respect to the collector and I is the current flowing through the diode. This expression arises from the product of two terms; the first is the effective emitter area which is proportional to $(V-V_p)$ and the second is the current density in a space-charge region which has been studied by Shockley and Prim (1953) and Dacey (1953). These papers are more fully discussed in chapter II.

1.4 Criteria for Selection of Transistors

(a) Avalanche multiplication of a current occurs when electrons or holes acquire sufficient energy from the field between collisions to ionize atoms, thus producing electron-hole pairs; breakdown occurs at a critical applied voltage. Experimentally this is noticed as a very rapid increase in current for a relatively small change in the applied voltage. Miller (1955) observed that the multiplication of minority carriers coming from the high resistivity side of a p-n junction followed the empirical form

$$M(V) = \frac{1}{1-\left(\frac{V}{V_B}\right)^z} \tag{1.4.1}$$

where M = the current multiplication factor,
         V = the voltage across the junction,
         V_B = the junction breakdown voltage, and
         Z = is a parameter depending on the resistivity and

resistivity type, of the high resistivity side of the junction.
For high resistivity n-type germanium, $z \simeq 3$.

Miller also observed an empirical relation between the
junction breakdown voltage V_B and the n-type impurity

concentration N ,

$$V_B = 1.0 \times 10^{13} \cdot N^{-0.725} \qquad (1.4.2)$$

where V_B is in volts and N in cm^{-3}.

Making use of equation (1.3.1) for the punch-through
voltage and the relation between the α cut-off frequency f_α
and the base width W

$$f_\alpha = \frac{0.4 \; D_p}{W^2} \qquad (1.4.3)$$

if the parameters f_α , D_p and V_p are known, it is possible
to determine W, N and V_B and thus determine the multiplication
factor M .

On the assumption that to avoid avalanche multiplication
effects it is necessary to have $(M-1) \ll (1-\alpha)$ where $\alpha = \frac{I - I_s}{I}$
and I is the current through the diode and I_s is the saturation
current of the reverse biased junction, Nichol (1958) derived
from the above formulae that

$$\frac{V}{V_B} \leqslant 0.1 \qquad or \qquad (V_p f_\alpha)^{0.725} V \leqslant 4 \times 10^7$$

where V, V_B are in volts and f_α is in sec^{-1}.

(b). Since it is desired to study body conduction, it is necessary that no surface conduction be present. The presence of surface conduction channels between the emitter and collector can be determined by observing the floating emitter potential, before punch-through. The emitter-base potential should be

$$V_{eb} = \frac{kT}{q} \ln(1-\alpha) \quad \text{for} \quad \frac{kT}{q} \ll -V_c < V_p \qquad (1.4.4)$$

where V_{eb} and V_{cb} are the emitter and collector voltages measured with respect to the base. Brown (1953) has found that surface conduction channels will lead to values of V_{eb} many times the above value.

1.5 Shot Noise

The two most important types of noise in semiconductors are shot and thermal noise. Shot noise occurs in a vacuum diode or in a transistor and is due to the drift current being composed of randomly emitted electrons. A spectral density analysis of the current fluctuations for shot noise yields for frequencies much less than the reciprocal of the transit time

$$S(f) = 2q |I| \qquad (1.5.1)$$

where $q =$ the electronic charge,
$I =$ the mean current, and
$f =$ the frequency.

Deviation from this law can occur when there is space-charge limitation of the current as discussed in detail by Thompson, North and Harris (1940-41). The potential distribution
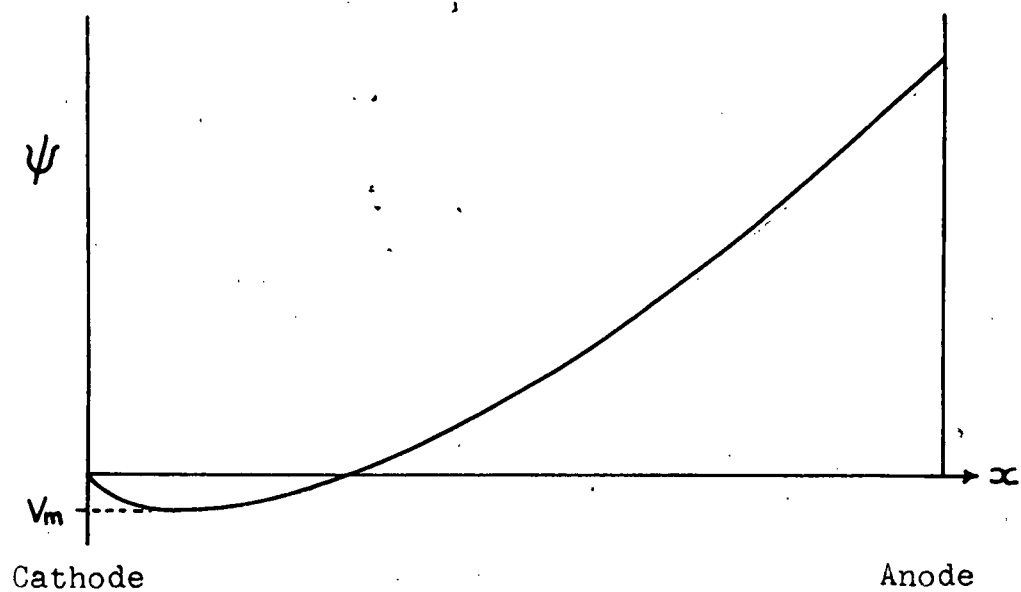
Figure 5a – Potential Distribution in a Vacuum Diode with a
Space-charge-limited Current
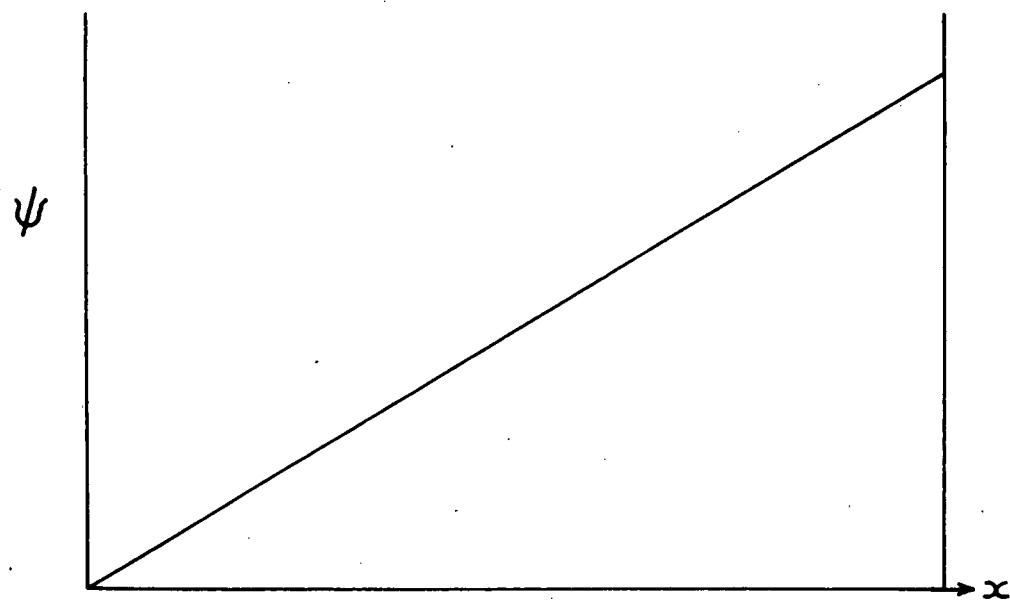
Figure 5b – Potential Distribution in a Vacuum Diode with a
Saturated Current

in a vacuum diode with a space-charge-limited current is shown in figure 5a; it can be readily seen that if at any time a larger number of electrons than average is emitted from the cathode, that this will cause a lowering of the potential minimum V_m, and, since the electrons are emitted with a Maxwellian velocity distribution, fewer than average will be able to pass through the lowered V_m. In a similar manner, a smaller emission rate increases V_m and increases the fraction of electrons passing the potential minimum. It is easy to see that such a process will lead to a reduction of the noise due to the random emission rate of electrons from the cathode. In a diode where there is no space-charge limitation, there is no V_m and all the emitted electrons go to the anode; such a diode is said to be saturated and it shows full shot noise. In general then

$$S(f) = 2q|I|\Gamma^2 \qquad\qquad (1.5.2)$$

where Γ = the space-charge reduction factor,
         $\Gamma \approx 1$ for a saturated diode, and
         $\Gamma < 1$ for a space-charge limited diode.

In practice it is possible to realize a Γ as low as 0.2 in a vacuum diode.

In a solid such as germanium, the situation is quite different; the electrons or holes undergo frequent collisions with the lattice vibrations, phonons, and for moderate electric fields, the velocity distribution of the current carriers is Maxwellian, with a comparitively small drift velocity superimposed
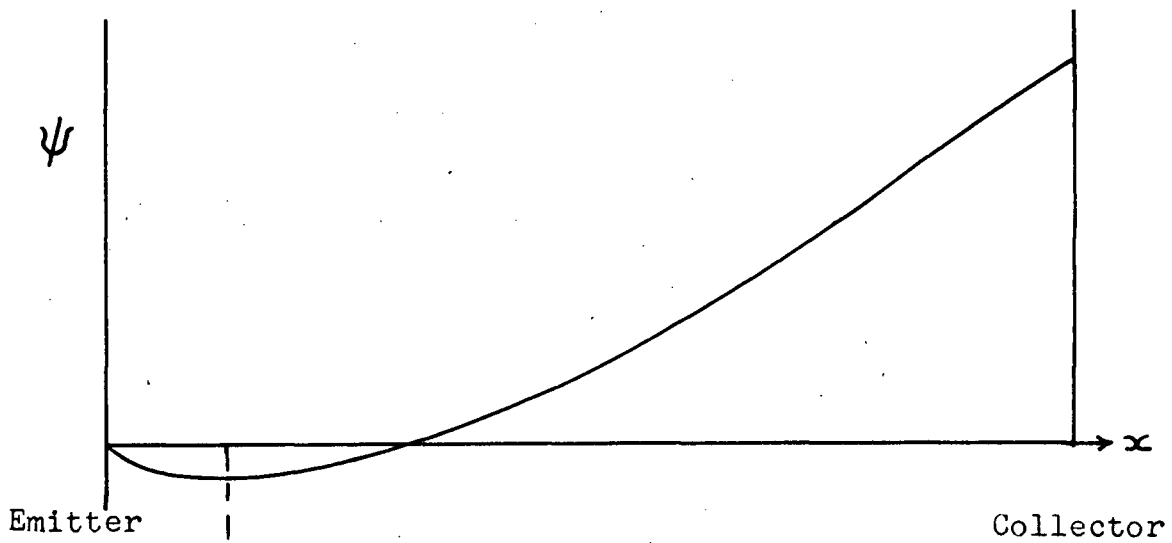
Figure 6a - Potential Distribution in the Depleted Base
Region of a P-n-p Diode
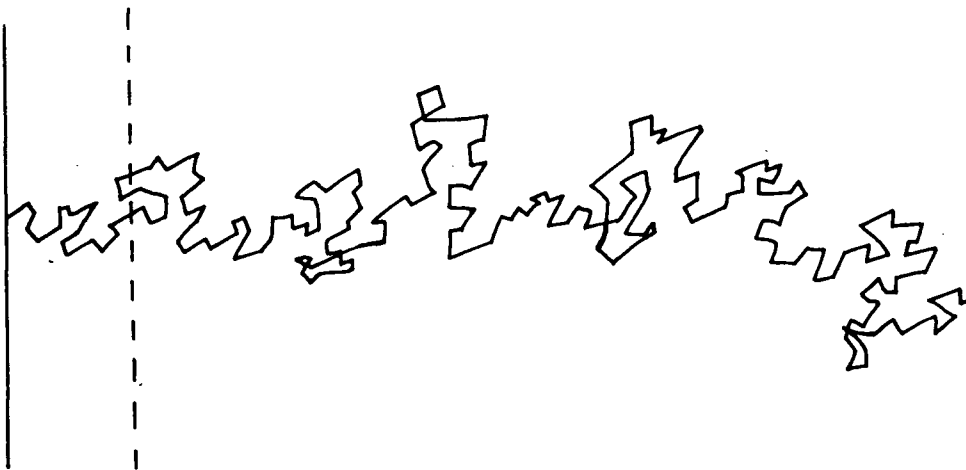
Figure 6b - Typical Path of a Hole across the Depleted Region
of the Base of a P-n-p Diode

$$p(\vec{v}) = \left(\frac{m}{2\pi kT}\right)^{3/2} \cdot \exp\left\{-\frac{m}{2kT}(\vec{v}-\vec{v_d})^2\right\} \qquad (1.5.3)$$

where $p(\vec{v})$ = the probability density of carriers with velocity $\vec{v}$,
m = the mass of a current carrier, and
$\vec{v_d}$ = the drift velocity.

The motion of a hole through the base region of a p-n-p transistor with the base depleted of majority carriers will appear similar to the example shown in figure 6. This situation is quite different from the vacuum diode in two respects; firstly the electric field is mainly due to the positive donor ions, and the holes contribute only close to the emitter; secondly the motion of the holes is mainly thermal and the electric field has only a minor effect on it. It is thus unlikely that small variations in the potential minimum will have sufficient effect on the holes to reduce shot noise appreciably, since the cooperative action of the potential fluctuations will be destroyed by the randomness and frequency of the scattering process.

1.6   Thermal Noise

Thermal noise currents occur in any substance and are caused by the thermal motion of the free carriers. The spectral density of the current fluctuations in a passive network is given by Nyquist's theorem,

$$S(f) = 4kTG(f) \qquad (1.6.1)$$

where k = Boltzmann's constant,
T = the absolute temperature of the network, and
$G(f)$ = the a-c. conductance of the network at frequency f.

Shockley (1951) has predicted that in germanium with an applied electric field, that the free electrons will not be in thermal equilibrium with the lattice, but will have much higher velocities than those given by the Maxwell distribution at the lattice temperature. The thermal noise due to these electrons can obviously not be evaluated on the assumption that the electrons are at the lattice temperature so it is convenient to ascribe to the electrons a value of temperature higher than that of the lattice, and in Appendix II it is shown that the appropriate noise temperature is given by

$$k T_n = m (\overline{u^2} - \overline{u}^2) \qquad (1.6.2)$$

where $m =$ the mass of a carrier,
$u =$ the velocity component of a carrier in the direction of the field, and

$T_n =$ the effective carrier noise temperature.

The mechanism leading to such a behaviour is briefly this that the carriers acquire energy from the electric field between collisions, and that they are unable to dissipate all this energy during a collision. The carriers gain more and more energy until they are on the average able to lose as much energy during a collision as they acquire between collisions. The Shockley paper and other relevant succeeding ones are more extensively reviewed in chapter II.

The noise in a current through a rectangular homogeneous solid with a uniform electric field distribution is evaluated in Appendix II and found to be

$$S(f) = 4kT_n G(f) + 2q|I| \qquad (1.6.3)$$

where the noise temperature T_n is given by equation (1.6.2).
Thus it is seen that the noise can be divided into shot and
thermal noise components, and that these can be discussed
separately.

Chapter II -- REVIEW OF PREVIOUS WORK

2.1   Diode Current for $V < V_P$

The current in an emitter-collector diode for voltages
less than the punch-through voltage has been studied by
Götzberger (1959). The current in such a diode with the
collector reverse biased is equal to

$$I'_{co} = \frac{I_{co}}{1 - \alpha} \tag{2.1.1}$$

where I_{co} is the reverse saturation current of the collector
junction and α is defined as $-\frac{\partial I_c}{\partial I_e}$ under common emitter
operation, I_e and I_c are the currents entering the emitter and
collector respectively. The above relation can be very easily
derived by considering the base current of the transistor; the
latter consists of the fraction $(1-\alpha)$ of the total current
entering the emitter, and the current $-I_{co}$ entering the
collector. Since in the diode connection the base is floating,
the total base current must be zero and $(1-\alpha)I'_{co} = I_{co}$;
equation (2.1.1) follows immediately.

Since the fraction of carriers emitted by the emitter that
are lost in the base due to surface recombination is equal to
the ratio of the base width W to the diffusion length L_s of the
carriers in the base, $(1-\alpha) = \frac{W}{L_s}$ and the following equation is
obtained for the total current:

$$I'_{co} = \frac{L_s}{W} I_{co} \tag{2.1.2}$$

Since no recombination can occur in the space-charge
region in front of the collector, the value of W in equation
(2.1.2) should be reduced accordingly. Using the condition that
the integration of the electric field over the space-charge
region gives the applied voltage V yields

$$I'_{co} = \frac{L_s I_{co}}{W} \frac{1}{1 - \sqrt{V/V_P}} \qquad (2.1.3)$$

Since this formula did not agree with experimental
observation Götzberger suggested that a further correction due
to non-planar geometry was needed and that a non uniform
base width would lead to a punch-through voltage varying
across the base. He proposed as a model of the transistor,
two transistors with different base widths in parallel; this
model gave

$$I'_{co} = \frac{L_s I_{co}}{W A} \left\{ \frac{A_1}{1 - \sqrt{V/V_{P_1}}} + \frac{A_2}{1 - \sqrt{V/V_{P_2}}} \right\} \qquad (2.1.4)$$

where A_1 and A_2 are the areas of the two transistors with
punch-through voltages V_{P_1} and V_{P_2}; also $A = A_1 + A_2$.

A most interesting case occurs when one of the junctions
has a projection into the base; such a projection will be
accompanied by a very small area and a small punch-through
voltage.. In such a transistor the current will be determined
mainly by the larger area transistor until the punch-through
voltage of the spike is reached. At this voltage the current
will increase very rapidly, and most of the current will occur
at the spike.

Equation (2.1.4) is illustrated graphically in figure 24

where a fit is made to current-voltage characteristics obtained experimentally.

2.2   Diode Current for $V > V_P$

Space-charge limited currents in germanium have been studied by Shockley and Prim (1953), Dacey (1953) and Nichol (1958).

Shockley and Prim analysed an n-i-n diode, and assuming that the drift current was much greater than the diffusion current, they obtained for the current density

$$J = \frac{9 \epsilon \mu_0 V^2}{8 W^3} \qquad (2.2.1)$$

where $V =$ the applied voltage,
$W =$ the base width, and
$\mu_0 =$ the electron mobility in the base, assumed to be
independent of the electric field.
Shockely and Prim also analysed a p-n-p diode, including the effect of the fixed donor charge density of the base, and again assuming the mobility to be field independent. This gave for high applied voltages a result similar to (2.2.1), but at lower voltages the current decreased more rapidly and for $V \le V_P, J=0$.

The effect of the variation of mobility with field on the above models was considered by Dacey (1953). The current density in a p-i-p diode with a field dependent mobility, $\mu \propto F^{-\frac{1}{2}}$, was found to be proportional to $V^{\frac{3}{2}}$ for voltages much greater than the punch-through voltage. For smaller voltages and current densities the effect of the fixed charge in the base, which can

never be completely eliminated, was not neglected and the Shockley and Prim results used. Good agreement between experimental and theoretical results was obtained.

Since the field in a p-n-p diode varies over a wide range across the base, Nichol (1958) considered the following velocity field relation which approaches the constant mobility case for low fields and the constant velocity V_0 at high fields;

$$V = \frac{\mu_0 F}{1 + \frac{\mu_0 F}{V_0}} \qquad (2.2.2)$$

where V = the carrier drift velocity,
F = the electric field strength, and
μ_0 = the zero field mobility.

Applying this to the p-n-p diode gives for the field distribution

$$F = \left\{ \frac{2V_P}{W^2} + \frac{J}{V_0 \epsilon} \right\} x + c \sqrt{\frac{J}{\mu \epsilon}} \sqrt{x} \qquad (2.2.3)$$

and for the current-density voltage relation

$$V - V_P = \frac{W^2 J}{2\epsilon V_0} + \frac{2c}{3} \left(\frac{W^3}{\epsilon \mu_0} \right)^{1/2} \sqrt{J} \qquad (2.2.4)$$

where C is a dimensionless parameter which varies slightly with the current density, and x represents the distance across the base from the emitter. A value of $C = 1.3$ gives less than 10% error over a field range of 500 to 14,000 volts /cm, and the limiting value of C for low fields is $2^{\frac{1}{2}}$. For the transistors used the two terms in (2.2.4) were equal at a current of 30 milliamperes: at lower currents the second term was predominant and at higher currents the first term was predominant.

For current densities $J \ll \frac{16 c^2 V_0^2 \epsilon}{9 \mu_0 W}$ the above equations give

$$F = \frac{2V_P}{W^2} x + C\sqrt{\frac{J}{\mu_0 \epsilon}} \sqrt{x} \qquad (2.2.5)$$

and

$$J = \frac{9 \epsilon \mu}{8 W^3} (V-V_P)^2 \qquad (2.2.6)$$

However to relate the current density to the current, the former must be multiplied by the effective area of the emitter. To explain his results, Nichol found it necessary to assume that the space charge region touches the emitter as a sphere touches a plane, the effective area was found to be

$$A = (V-V_P) \frac{\pi W^2}{V_P} \qquad (2.2.7)$$

Combining this with (2.2.6) yields for the total current

$$I = \frac{9 \pi \epsilon \mu_0}{8 V_P W} (V-V_P)^3 \qquad (2.2.8)$$

For a transistor with non-planar geometry, an additional current will flow from that part of the emitter which is not in contact with the space-charge region, this current will be a diffusion current such as discussed in section 2.1.

2.3   Shockley and Hot Electrons

There are two problems considered by Shockley (1951) in evaluating the equilibrium state for electrons subjected to an electric field in germanium. They are the physical mechanism of the interactions between electrons and phonons, and the condition at which a steady state exists.

A phonon is a quantum of energy of one of the normal modes of lattice vibration, and in the diamond type lattice of germanium there are two different types of modes characterized by different frequency wavelength relationships. The acoustical modes are characterized by the relation $\lambda\nu = s$ where λ and ν are the wavelength and frequency respectively; s is the velocity of sound and deviates from a constant only at wavelengths of the order of the interatomic distance. The optical modes are characterized by a frequency ν_{op} which is very nearly independent of wavelength. Since the energy of an optical phonon in germanium is $h\nu_{op} = kT_{op}$ where $T_{op} = 520°K$ and k is Boltzmann's constant, the probability that a particular optical mode is excited is small for a lattice at room temperature.

Shockley first considers collisions between electrons and acoustical modes only; the mechanics of a collision are calculated by using the laws of conservation of energy and momentum. By considering the various transition probabilities he shows that the scattering of electrons by acoustical phonons is analogous to the scattering of a small electron mass m by a large equivalent phonon mass $M_0 = \dfrac{kT_0}{s^2}$, moving with a thermal energy appropriate to the lattice temperature T_0 . The average energy gain per collision for an electron with an initial momentum P_1 is $\left(\dfrac{4mkT_0}{M_0} - \dfrac{P_1^2}{M_0}\right)$. Assuming the electron velocity distribution to be Maxwellian with an r.m.s. velocity v_E, the average rate of energy gain of an electron due to phonon interaction is

$$\left(\frac{dE}{dt}\right)_{phonons} = \frac{8}{\sqrt{\pi}} \frac{ms^2 v_E}{\ell} \left\{ 1 - \left(\frac{v_E}{v_T}\right)^2 \right\} \qquad (2.3.1)$$

where ℓ, the mean free path, and $v_T = \sqrt{\frac{2kT_0}{m}}$ have been introduced.

The electron acquires energy from the field F at a rate

$$\left(\frac{dE}{dt}\right)_{field} = q v_d F \qquad (2.3.2)$$

where v_d is the drift velocity.

In the steady state the average rate of energy change of an electron must be zero, and (2.3.3) is obtained when this condition is applied to the previous equations.

$$\frac{T_e}{T_0} = \left(\frac{v_e}{v_T}\right)^2 = \frac{1}{2}\left\{1 + \left\{1 + \frac{3\pi}{8}\left(\frac{\mu_0 F}{s}\right)^2\right\}^{1/2}\right\} \qquad (2.3.3)$$

where the zero field mobility μ_0 is introduced and T_e is the effective electron temperature defined by $kT_e = \frac{1}{2}m v_e^2$. This gives two limiting forms for the drift velocity and effective electron temperature:

$$\text{for} \quad F \ll F_0 , \quad v_d = \mu_0 F \qquad \frac{T_e}{T_0} = 1 + \left(\frac{F}{F_0}\right)^2$$

$$(2.3.4)$$

$$\text{for} \quad F \gg F_0 , \quad v_d = \mu_0 \sqrt{F F_0} \qquad \frac{T_e}{T_0} = \frac{F}{F_0}$$

where F_0 is the field at which the two limiting forms for the drift velocity are equal, $F_0 = \frac{s}{\mu_0}\left(\frac{32}{3\pi}\right)^{1/2}$.

These results agree qualitatively with the experimental mobilities obtained by Ryder (1953), Arthur Gibson and Granville (1956), and Larrabee (1959), but the critical field F_0, at which the drift velocity changes from an F law to an $F^{1/2}$ law, is observed to be three times greater than predicted. Shockley attributes this discrepancy to the fact that the electron mass is not single valued and shows that this leads to a greater

efficiency of energy transfer and a constant mobility up to higher fields.

Since the optical modes are almost unexcited at room temperature, they cannot give energy to the electrons, however they can absorb energy. This can only occur when an electron has a kinetic energy greater than $h\nu_{op}$, the energy of an optical phonon, a situation which rarely occurs at low fields. In an electric field high enough so that an electron gains an energy $h\nu_{op}$ between collisions, optical mode scattering becomes very important and is very much more efficient than acoustical mode scattering because of the much larger energies transferred. A simple analysis, assuming that an electron is accelerated from rest until it gains an energy $h\nu_{op}$ and then loses it to an optical mode, leads to a drift velocity independent of the electric field, $v_d = \left(\dfrac{h\nu_{op}}{2m}\right)^{1/2}$.

Such a simple treatment completely neglects acoustical mode scattering, the relative mean free paths for acoustical and optical mode scattering, and the probability that an electron may acquire more energy than $h\nu_{op}$ before being scattered. Shockley considers these in a more general analysis which predicts a constant mobility at low fields, a drift velocity proportional to $F^{1/2}$ at intermediate fields, a saturation drift velocity at high fields and a further increase in drift velocity at even higher fields. By using an experimental value of the low field mobility and adjusting the velocity of sound, Shockley obtains good numerical agreement between his theory and experimental data for the drift velocity up to a field of

30,000 volts/cm. He estimates the effective electron temperature
to be 4000°K at this highest field and 1000°K at a field of
8,000 volts/cm. It should be noted that these temperatures are
three times lower than those predicted by equation (2.3.4), the
difference being due to the inclusion of the optical modes as
a scattering mechanism.

2.4   Further Work

A review of recent theoretical and experimental work on
warm and hot electrons is given by Koenig (1958).

The energy distribution function for electrons in
germanium was calculated by Yamashita and Watanabe (1954) for
acoustical mode scattering, and the analytical expression
obtained was the Pisarenko distribution

$$N(E) = N_0 \cdot E^{1/2} \left(\frac{E}{kT_0} + p \right)^p \exp\left(-\frac{E}{kT_0} \right) \qquad (2.4.1)$$

where N_0 = a constant,
         E = the electron energy,
         T_0 = the lattice temperature, and

$$P = \frac{q^2 \ell^2}{6 m s^2 k T_0} F^2$$

where q = the electronic charge,
         ℓ = the mean free path at low fields,
         m = the effective mass of a conduction electron,
         s = the velocity of sound, and
         F = the electric field strength.

Using the experimental value for the zero field mobility, they
calculated the proportionality constant between p and F^2 and
subsequently the mobiliity at higher fields. The results were
in substantial agreement with those of Shockley. The noise

temperature to be expected on the basis of these results is
calculated in section 4.3. Yamashita and Watanabe also consider
the effects of optical mode scattering and obtain results in
good agreement with Shockley; their consideration of the effects
of impurity scattering indicate a reduction in the critical
field for large impurity concentrations at which the mean free
path due to the impurities is of the same order of magnitude
as that due to phonons.

Frohlich and Paranjape (1956) showed that when the free
electron density is sufficiently large that inter-electronic
collisions determine the velocity distribution function which
will be Maxwellian displaced by the drift velocity in the
direction of the electric field. On this basis, Stratton (1958)
calculated the velocity field relation for germanium at room
temperature and obtained good agreement with the experimental
results of Arthur, Gibson and Granville (1956). The main
difference between this analysis and the previous ones is that
the effect of the optical modes is considered for fields at
which the mean electron energy is less than $h\nu_{op}$.

Gunn (1957) considers the effect of optical mode scattering
with a simple model, based on Shockley's elementary treatment
which leads to a drift velocity independent of the field. The
model is that an electron always moves in the direction of the
applied field with the following probabilities of being
scattered:

$$
\begin{cases}
0 & \text{for} \quad u < \nu_{op} \\
a\,(u - \nu_{op})^b & \text{for} \quad u > \nu_{op}
\end{cases}
\qquad (2.4.1)
$$

where a and b are constants, u is the electron velocity and $v_{op} = \left(\frac{2hv_{op}}{m}\right)^{1/2}$. The value of b is related to the effectiveness of the optical modes as a scattering mechanism; a value of $b \gg 1$ means that as soon as an electron reaches an energy hv_{op}, it is scattered and starts again from zero energy. Clearly in this case the drift velocity and mean square velocity are given by

$$u_d = \frac{1}{2} v_{op} \quad \text{and} \quad \overline{u^2} = \frac{1}{3} v_{op}^2. \qquad (2.4.2)$$

Gunn calculates the drift velocity for non-infinite values of b, and finds that this gives a rise in the drift velocity at high fields. The mean kinetic energy of an electron is then $\overline{E} = \frac{1}{2} m \overline{u^2} = \frac{1}{3} hv_{op}$, for $b \to \infty$, and if the effective electron temperature is defined in analogy to that for a Maxwell distribution, $\overline{E} = \frac{1}{2} k T_e$ for one dimension, the value $T_e = \frac{2}{3} \frac{hv_{op}}{k}$ is obtained. Substituting the value $hv_{op} = k T_{op}$ and $T_{op} = 520^\circ$K yields $T_e = 340^\circ$K.

It should be noted that in this model the results are quite independent of the lattice temperature whereas the experimental results of Ryder (1953) show that the saturation drift velocity decreases with increasing lattice temperature. The effective electron temperature is in sharp disagreement with that predicted by Shockley (1951) and Yamashita and Watanabe (1954) of about 4000°K. In section 4.3 it is shown that when the effective noise temperature is considered the disagreement is even greater.

Chapter III -- EXPERIMENTAL INVESTIGATION

3.1 Selection of Transistors

The transistors chosen for this study were subjected to
tests for avalanche multiplication, inhomogeneity of the base
impurity density, and surface conduction. Since it was desired
to have transistors with step junctions and not diffused
junctions, so that the base would be homogeneous, only alloy
junction transistors were chosen. The Schenkel-Statz punch-
through voltages were measured and only those transistors
which were symmetrical with respect to emitter and collector
were chosen; transistors with poorly defined punch-through
voltages were rejected. The method used to determine the extent
of avalanche multiplication was that devised by Nichol (1958)
based on the work of Miller (1955) and the resulting criterion
used was that $(V_P/V_B) < 0.1$, where V_B is the collector breakdown
voltage. The Brown (1953) test was used to determine the extent
of surface conduction. The floating emitter potential was
measured and compared to the value obtained from equation (1.4.4)
using the measured value of α, only those transistors which
showed good agreement were chosen.

The only transistor type which was found acceptable in all
these respects was the General Electric 2N137, and individual
units were selected to meet the Schenkel-Statz and Brown tests'
requirements. Typical values for the 2N137 were $V_P = 6.0$ volts,

$$I \propto (V - V_P)^3$$
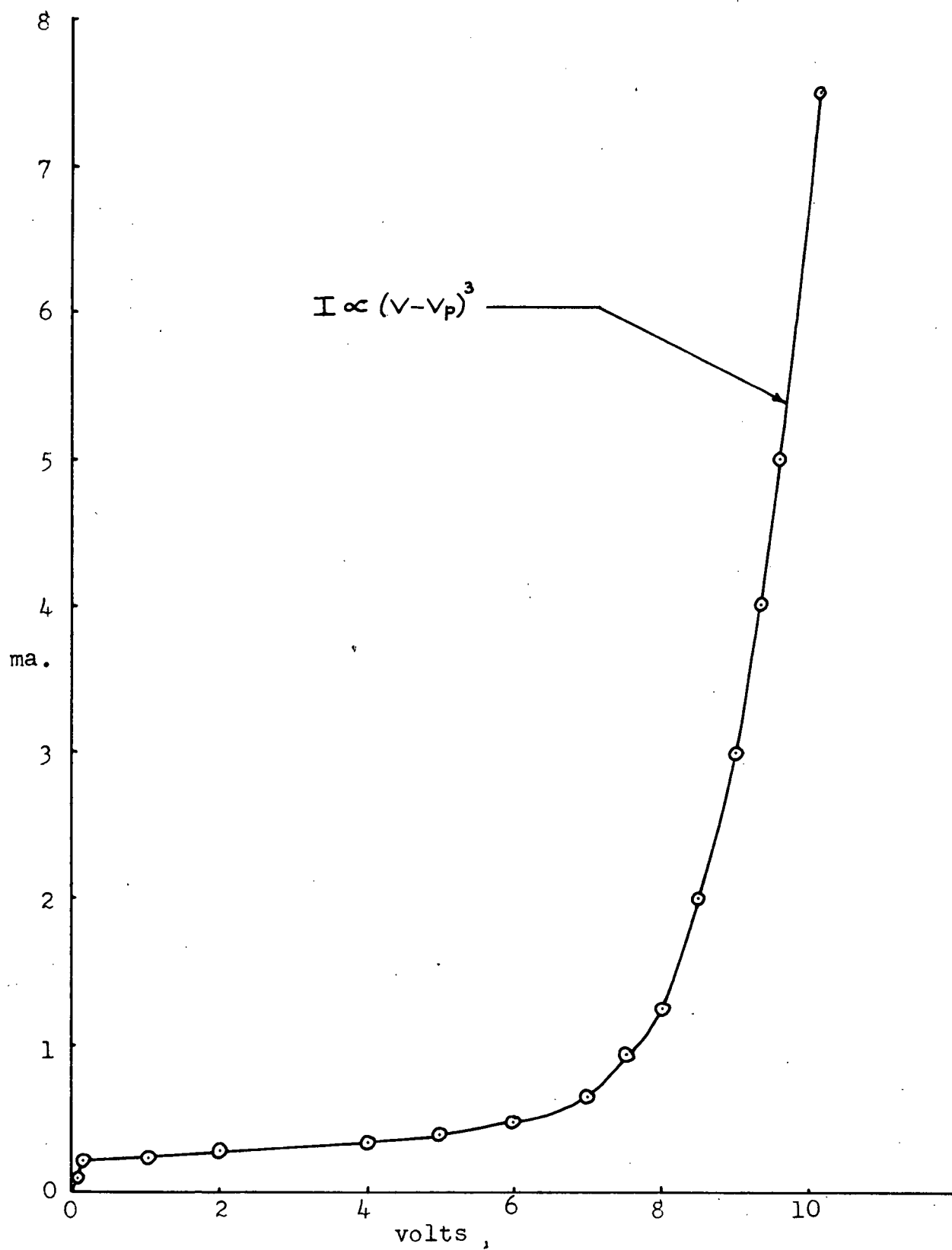
Figure 7 - D-C. Current-Voltage Characteristics of 2N137 #21

V_B = 60 volts, α = 0.98, and a floating emitter potential of 0.10 volts.

The dissipation coefficient in air for these transistors according to the manufacturer's data is typically 0.6 $^\circ$C per milliwatt, which at typical operating conditions of 10 volts and 5 milliamperes, would lead to a temperature rise of 30 $^\circ$C! It was thus found necessary to perform all the experiments with the transistor immersed in oil and with copper fins attached to all three leads. A thermometer in thermal contact with the base lead indicated a temperature rise of no more than 1°C under extreme operating conditions.

3.2   D-C. Characteristics

The emitter-collector d-c. current-voltage characteristics were measured with a milliameter and a high impedance voltmeter. Figure 7 shows a typical curve, which could be divided into two distinct regions of voltage. For voltages greater than the punch-through voltage it was found that

$$I \propto (V - V_P)^3 \qquad\qquad (3.2.1)$$

and for voltages below punch-through an empirical expression for the current was discovered to be

$$I - I_0 \propto V \qquad\qquad (3.2.2)$$

where I_0 was a constant. Equation (3.2.1) was in agreement with the results of Nichol (1958) except for the proportionality constant.

Figure 8 — Low Frequency Bridge
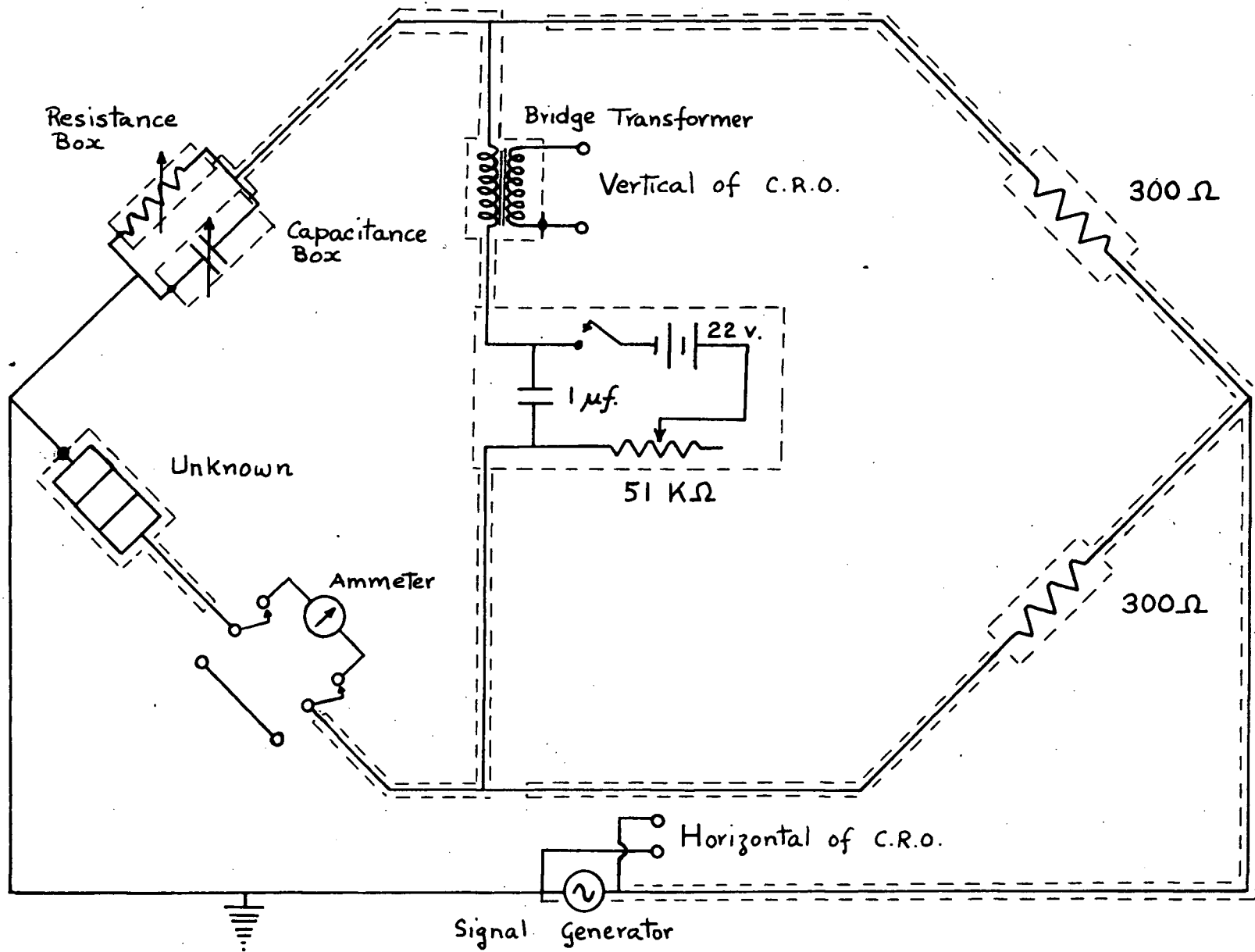
3.3   Low Frequency A-C. Characteristics

A Wheatstone type bridge was constructed for the
measurements of 'the a-c. admittance of the emitter-collector
diode between 1 kc/s and 500 kc/s. Available commercial
equipment could not be used since a very large condenser of
about 1000 μF would be needed to bypass the d-c. supply for the
transistor. To avoid this problem, the d-c. supply was
incorporated in the detector arm of the bridge, where it could
not affect the balance. The circuit is shown in figure 8 and
was found to have excellent sensitivity at the high frequencies
but was insensitive to capacitance changes below 20 kc/s. An
oscilloscope was used as the null detector, the horizontal
sweep being supplied directly from the oscillator. For a linear
device such as a resistor as the unknown the trace on the
oscilloscope was an ellipse, which became a horizontal line at
the null point; for a non linear device such as a transistor,
the second harmonic also appeared and a symmetrical figure-of-
eight indicated the balance point.

It was found that without the very carefully planned
shielding shown in the diagram the oscilloscope trace was
blurred due to 60 cps. pick-up and that it was impossible to
obtain a null. The limit on the sensitivity of the bridge was
placed by the gain of the oscilloscope and small amounts of
stray pick-up which occurred in spite of the shielding. The
former limit was necessitated by the non-linearity of the
transistor, because even small signal voltages displaced the
d-c. operating point of the transistor; this was observed by

Transistor
in
Oil Bath

1KΩ

·01 μf.

15 V.

Signal Generator   Wayne Kerr Bridge   Receiver
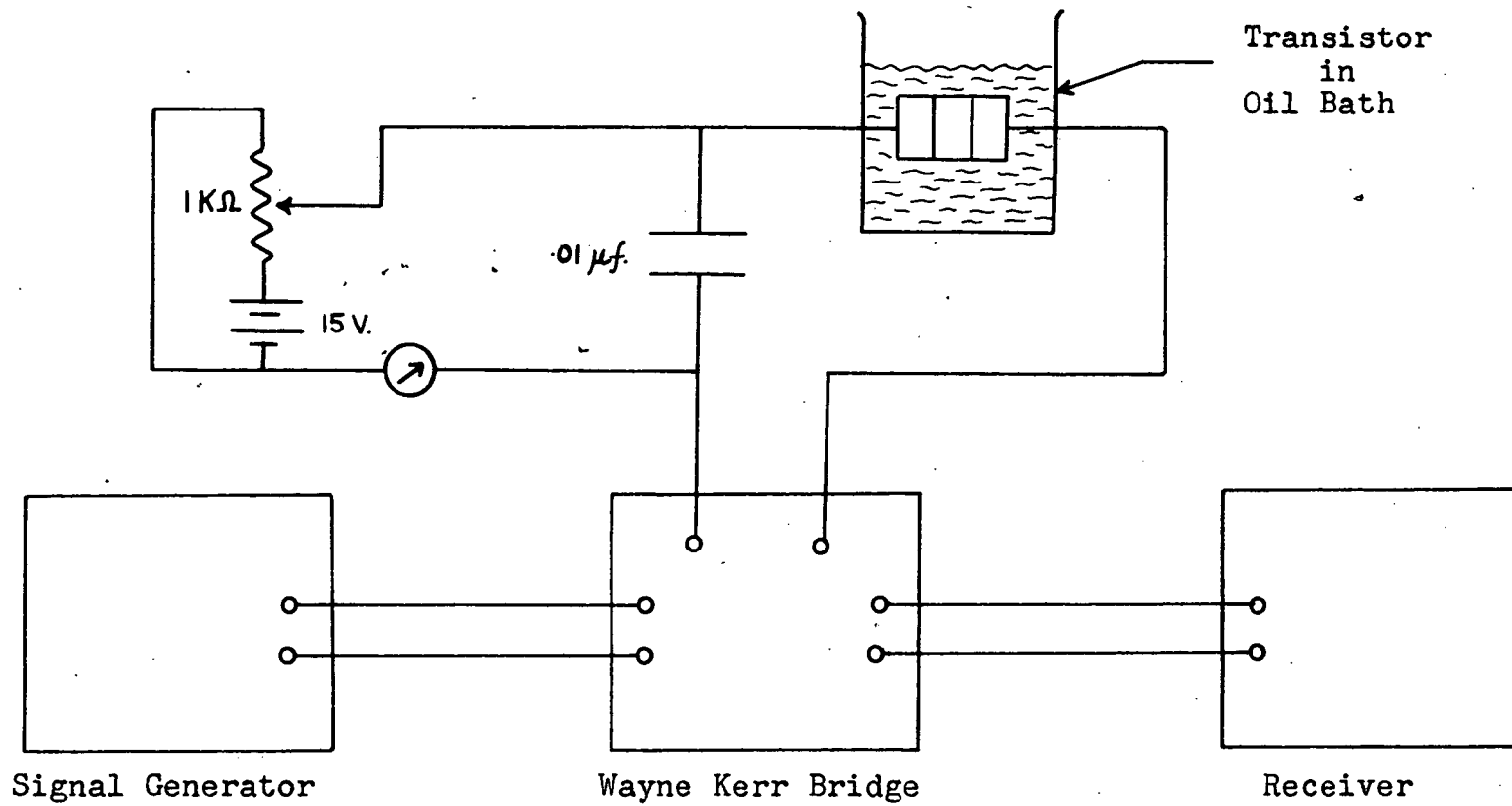
Figure 9 - Bridge Circuit for Measuing Transistor Impedance between 0.5 and 5 mc/s.

a change in the current and the appearance of higher harmonics on the oscilloscope. Care was taken to ensure that no appreciable displacement occurred; this was found to be very exacting at the lower currents, and in some cases meant that only one significant figure could be obtained.

The capacitance zero of the bridge was determined by substituting a carbon resistor as the unknown. For the range of frequencies used in the experiments, the overall variation was less than 200 pf., which was almost entirely due to the Shallcross resistance box used; the variation was less than 20 pf. between 20 and 500 kc/s.

The accuracy of the bridge was better than 5% over the resistance and capacitance ranges used.

3.4   High Frequency A-C. Characteristics

The diode admittance between 500 kc/s and 5 mc/s was measured with a model B 601 Wayne-Kerr bridge. The circuit used is shown in figure 9; the 0.01 μF condenser was effectively a short circuit at these frequencies and did not produce any unwanted resistance or capacitance components which it did at the lower frequencies, necessitating the construction of the bridge previously discussed. Measurements were made on carbon resistors, substituted for the transistor, to confirm that the bridge was working correctly.
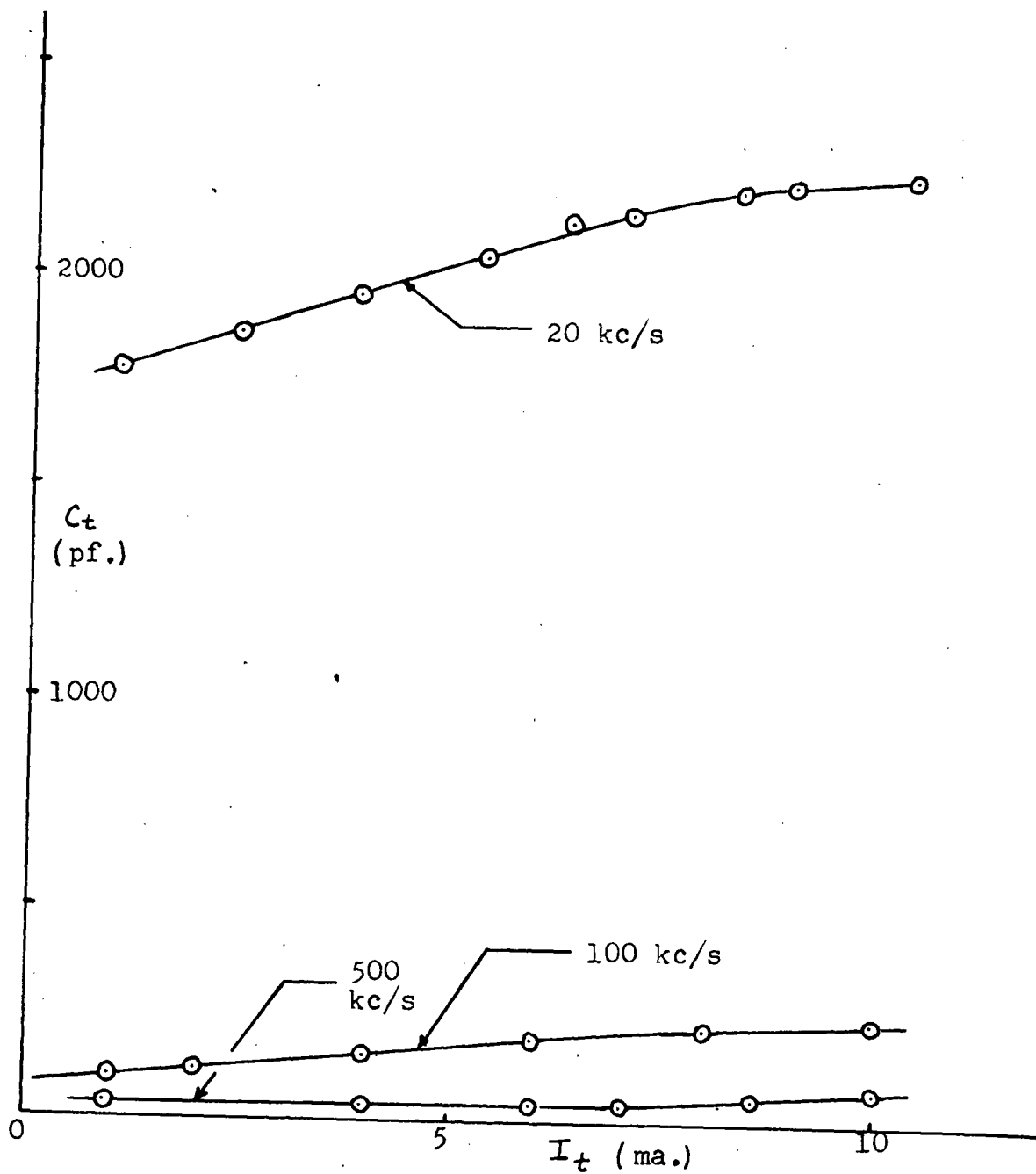
Figure 10 — Variation of Capacitance with Current for 2N137 #53

3.5   Experimental Impedances

Both bridges gave the effective a-c. impedance of the
transistor as an effective a-c. admittance $\frac{1}{R_t} + j\omega C_t$ where
R_t and C_t are the values of resistance and capacitance read off
the bridges. In this manner the transistor is represented as a
resistance R_t and a capacitance C_t in parallel.

Typical results obtained for the variation of R_t and C_t
with frequency and current are shown in figures 10,11,12 and 13
and some were quite unexpected, particularly the capacitance
rise at low frequencies which in some transistors reached 3000 pf.
The capacitance was found to be constant at low frequencies, and
to decrease as $f^{-3/2}$ from 100 kc/s to 1 mc/s. The differential
resistance R_t was observed to be constant above 200 kc/s, but to
rise at lower frequencies.

The variation of R_t with current is shown in figure 13 and
the 1 kc/s curve is seen to be similar to the derivative of the
d-c. characteristics. The capacitance was found to vary linearly
with the current between 1 and 6 milliamperes, with deviations
occurring at higher current as shown in figure 10.

3.6   Noise Measurements 20 to 500 kc/s

The principle used in all the noise measurements was that
of comparing the transistor noise with that of a standard noise
diode. The circuit used for frequencies between 20 and 500 kc/s
is shown in figure 14 and its equivalent circuit is shown in
figure 15. The extensive filtering used on the Transpac was

600

400

R_t
(ohms)

200

0

0   200 f (kc/s) 400   600

1.4 ma.

5.8 ma.

<u>Figure 11</u> — Variation of Resistance with Frequency for 2N137 #53

Figure 12 - Variation of C_t with Frequency for 2N137 no.53 at 3.0 ma.

$C_t \propto f^{-3/2}$
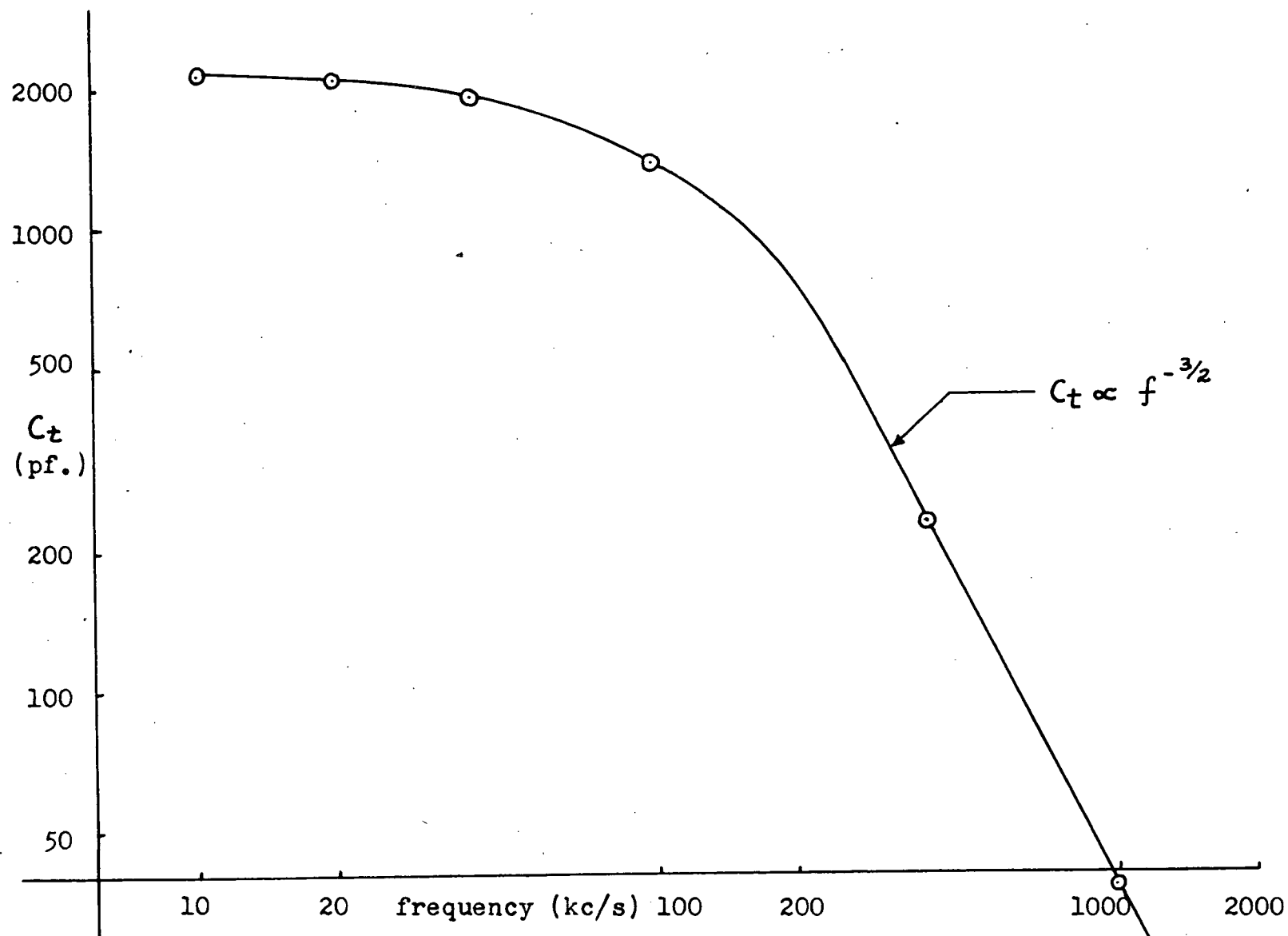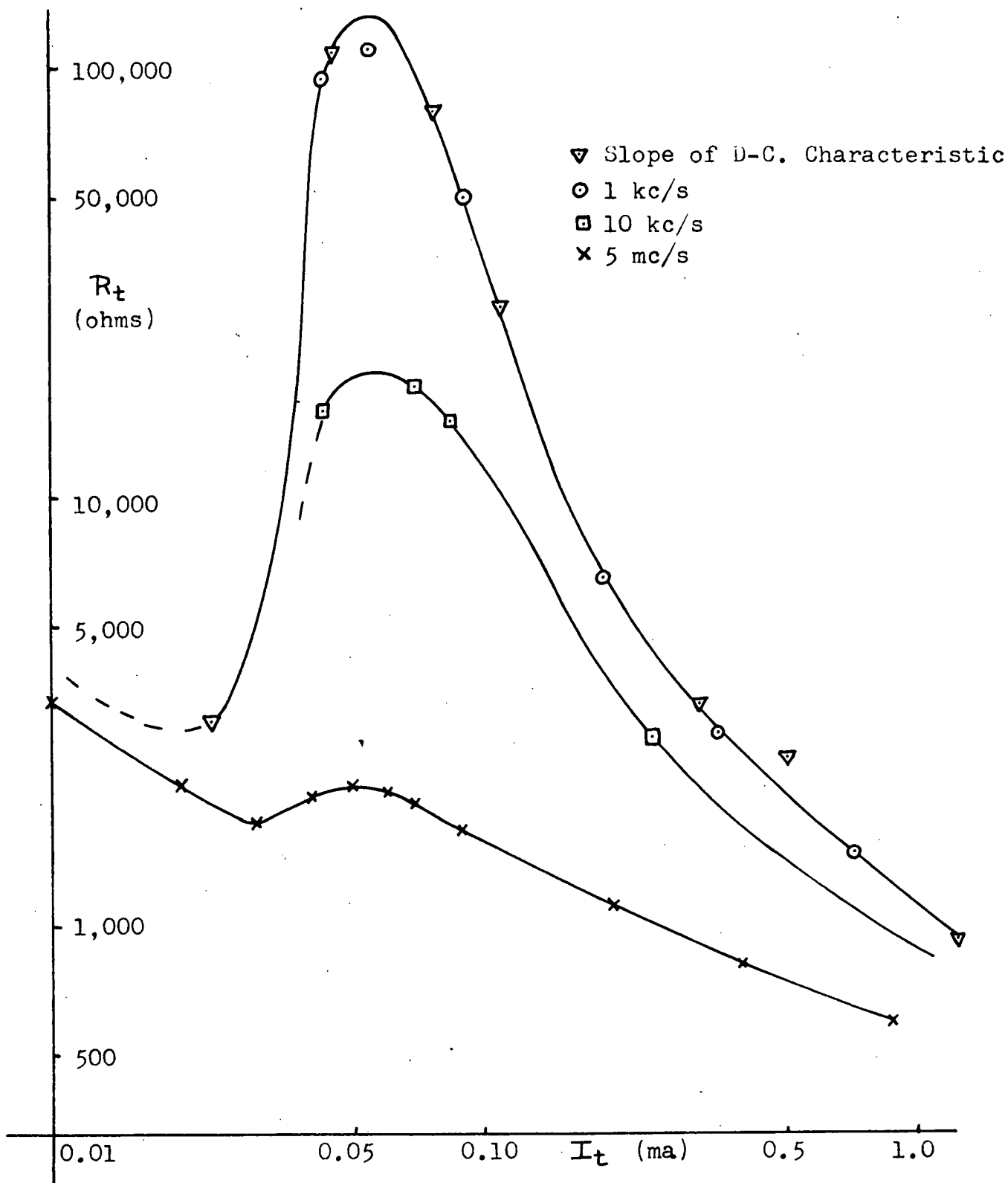
<u>Figure 13</u> — Variation of Transistor Resistance with Current for 2N137 #21

necessary to reduce the level of 120 cps. introduced via the
temperature variations of the diode heater. Additional filtering
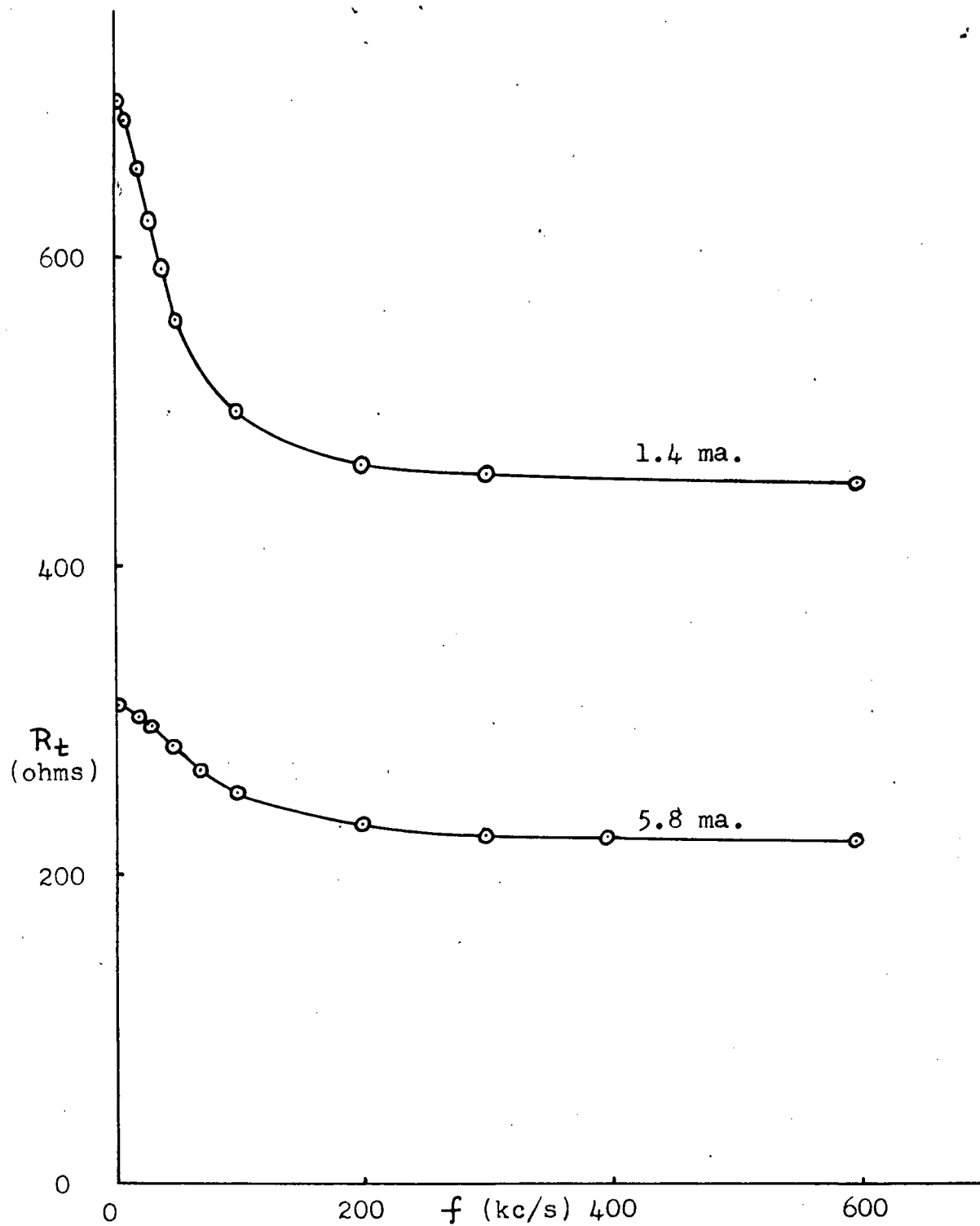was also found necessary between the two amplifiers to eliminate
stray pick-up from the rest of the circuit and amplified by the
first amplifier. No 60 cps. or 120 cps. could be detected with
an oscilloscope at the input of the wave analyzer. The noise
diode used was a Sylvania 5722, designed to generate full shot
noise under temperature-limited conditions as given by
equation (1.5.1).

The procedure for measuring the transistor noise was as
follows; with zero diode current, but a transistor current I_t
flowing, the output voltage was read on the wave analyzer. The
reading was then increased 3 db. by adjusting the diode filament
supply and the corresponding plate current I_d read. The
transistor noise was then represented as a shunt noise generator
of value $\overline{i^2} = 2q\,i_t\Delta f$ where $\overline{i^2}$ was the measured noise current
and the equation defines i_t. For negligible amplifier noise, the
procedure described above immediately gave $i_t = I_d$ since gain,
bandwidth and impedance did not vary between the measurements.

Three departures from this simple analysis were encountered,
in the measurements; the variation of diode conductance with
current, thermal noise generated by the load resistors, and the
amplifier noise. The diode conductance was measured at various
frequencies and currents and the highest value obtained was
20 μmho: this value was not large enough to cause any appreciable
error. The noise of the load resistors R_L was minimized by
using wire wound resistors, which exhibit only thermal Nyquist
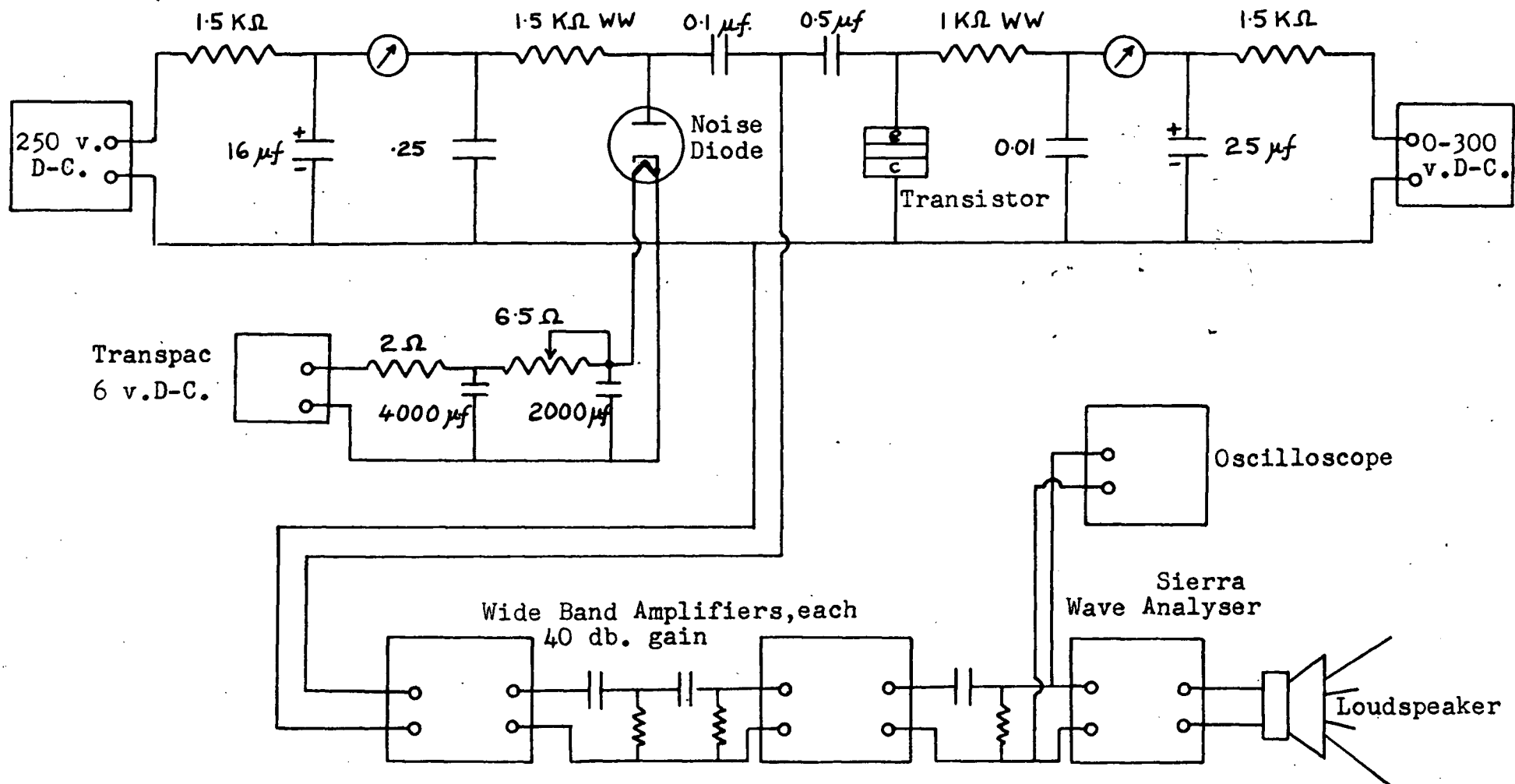
Figure 14 – Circuit Used for Noise Measurements between 20 and 500 kc/s.

noise. For the value $R_L = 600\Omega$ used, they had an equivalent shot

noise current of 0.1 ma. which was negligible compared with the

noise currents measured. All the results were corrected for the

amplifier noise, which was sometimes half of the total measured

noise. The amplifier noise was measured by a process identical

to the procedure for measuring the transistor noise except that

the transistor was disconnected; this gave an equivalent

amplifier noise current I_n which had to be corrected when the

transistor was in the circuit, due to the impedance change.

An analysis of the equivalent circuit shown in figure 15 gave

for the equivalent transistor noise current

$$i_t = I_d - I_n \left\{ 1 + \left(\frac{R_L}{R_t} \right)^2 \right\} \qquad (3.6.1)$$

where I_d = the anode current of the noise diode,
$1/R_L$ = the conductance of the load resistors,
$1/R_t$ = the incremental conductance of the transistor, and
I_n = the equivalent amplifier noise current with the

transistor disconnected.

In the above analysis the amplifier noise is assumed to be

equivalent to a constant voltage source at the amplifier input

terminals of value v_a^2 and the above representation by I_n is

merely a convenience; the two quantities are related by

$v_a^2 = 2q I_n R_L^2 \Delta f$ where Δf is the bandwidth of the measuring

circuit.

The value of R_L was calculated from the d-c. resistances

of the two load resistors and found to be $600\,\Omega$. The impedance

of the whole circuit as seen by the first amplifier was

measured with both bridges; they gave similar results of

$R_L = 600 \pm 5\,\Omega$ from 20 to 500 kc/s and an effective parallel
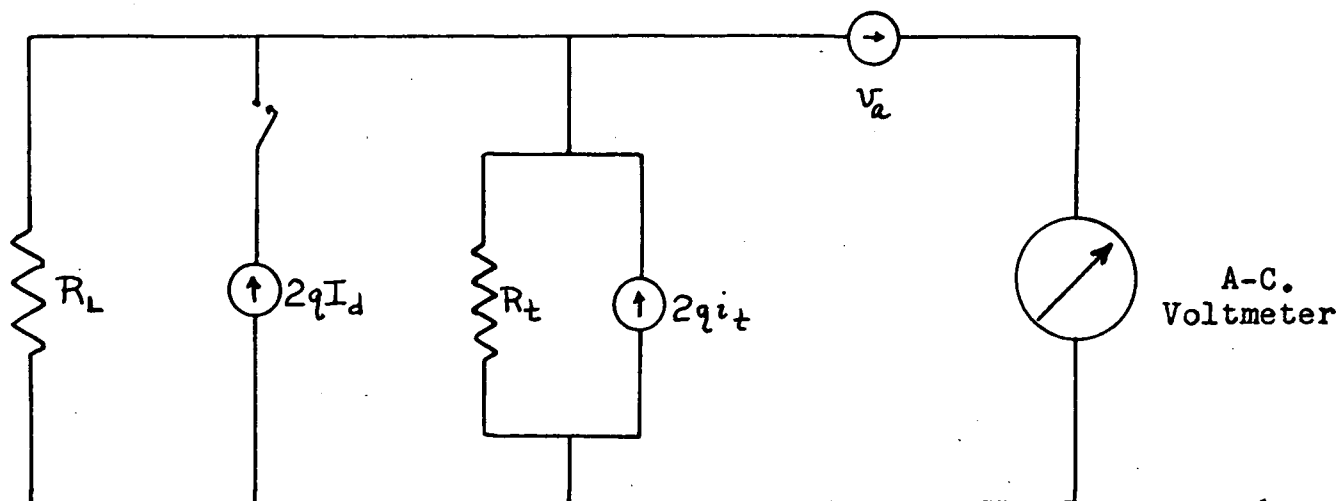
where R_L represents the transistor and noise diode load resistors, and R_t is the reciprocal of the transistor conductance at the frequency of the measurements.

Figure 15 - Equivalent Circuit of Noise Measuring Equipment of Figure 14

capacitance of 100 ± 15 pf. between 100 and 500 kc/s , rising
at lower frequencies due to the finite size of the coupling
capacitors. These measurements indicated that there were no
unknown conductances in the circuit, and that the equivalent
circuit was as shown in figure 15.

The variation of the square of the output voltage versus
the noise diode current was determined over a wide current
range and found to be an excellent straight line. This
procedure checked that the noise diode was delivering noise
$\overline{i^2} \propto I_d$, that the amplifiers were linear at the voltage levels
used, and that the output meter behaved as an r.m.s. meter for
noise. It is exceedingly unlikely that the amplifiers, diode
and meter would have compensating errors. Periodically, however,
a second noise diode was substituted for the original but no
change was found in the results. That the diode was in the
saturated condition necessary for the production of full shot
noise was periodically checked by observing the change in the
diode current with anode voltage. This was typically about
0.5 ma. per 50 volts, or a conductance of 10 μmhos at a plate
current of 15 ma. and it was very much smaller at smaller
currents; much larger conductances would have indicated that the
diode was unsaturated.

Another check of the operation of the circuit was made by
substituting a second noise diode in place of the transistor
and measuring its noise. The values of equivalent noise
currents agreed within 1.0 ma. from 0 to 30 ma., this was
repeated with similar results when the noise diodes were
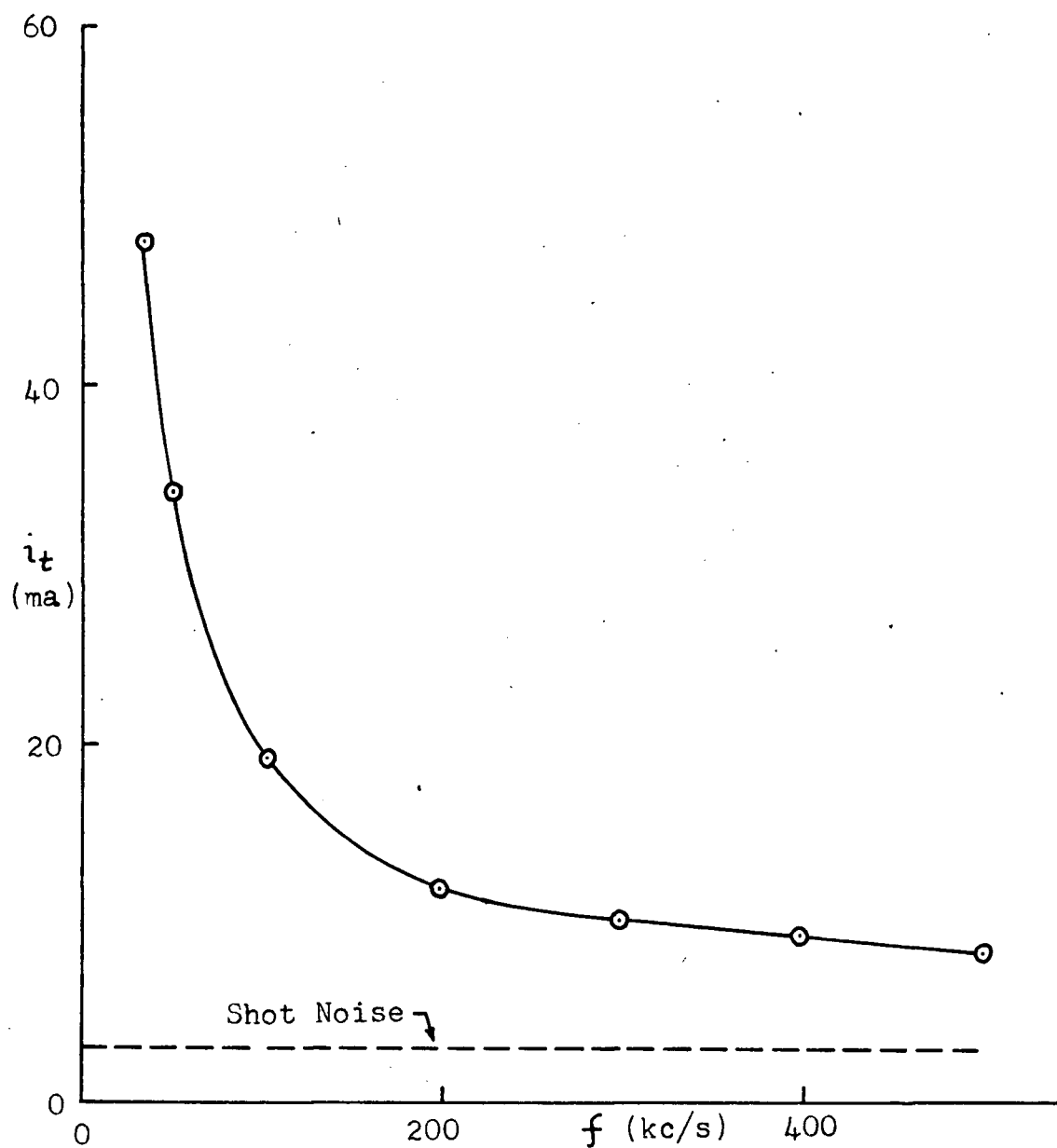
Figure 16 - Variation of Transistor Noise with Frequency at 3.0 ma. for 2N137 #53

interchanged.

Because of the very nature of noise, the meter on the
wave analyzer exhibited fluctuations, which were smoothed by
a 6000 μF condenser placed across the meter. This reduced the
meter fluctuations considerably, but increased the length of
time necessary for the meter to attain its correct mean value.
The condenser used provided a good compromise between these
effects, but the meter still had an overall fluctuation as much
as 0.5 db.; the ability to estimate the mean value of the meter
reading was the main limit on the accuracy of the experimental
results.

Typical results for the variation of transistor noise
with current and frequency are shown in figures 16 and 18. The
very rapid rise of noise at low frequencies and high currents
was attributed to excess or 1/f noise and it was apparent that
this was still present at 500 kc/s. As a consequence of this
it was decided that measurements should be made at higher
frequencies.

3.7   Noise Measurements at 5 mc/s

These were made with the circuit of figure 14 unchanged
except that the amplifiers and wave analyzer were replaced by
an Airmec receiver and an a-c. voltmeter. In addition all the
leads in the noise producing part of the circuit were shortened
to a minimum.

The equivalent circuit for this set up is shown in
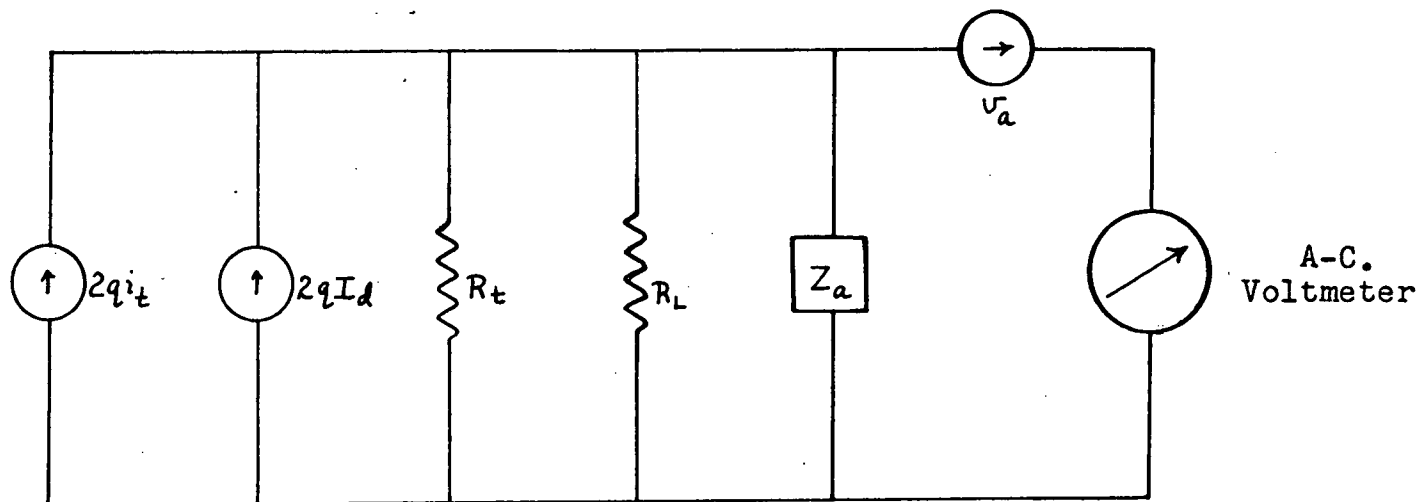
Figure 17 - Equivalent Circuit of Noise Measuring Equipment at Radio Frequencies

figure 17. Z_a represents the complex input impedance of the receiver. Because of the nature of Z_a, a new procedure for noise measurement was devised, consisting of three readings. The first reading was taken with the transistor disconnected and zero diode current, the second with the transistor connected and the desired current flowing, and the third with an additional diode current I_d flowing. With these three readings denoted by V_0 , V_1 and V_2 respectively, an analysis of the circuit gives

$$i_t = I_d \left\{ \frac{V_1{}^2 - V_0{}^2}{V_2{}^2 - V_1{}^2} \right\} \qquad (3.7.1)$$

Two possible sources of error were present here; the conductance of the noise diode was again present but negligible, however the variation of the noise of Z_a with external damping was found to be not negligible. This variation was determined by substituting carbon resistors for the transistor and the appropriate corrections were made to V_0 .

This method had the additional advantage that it was not necessary to know the value of R_t, or to adjust the diode current to meet a predetermined condition. In general a diode current was used that gave $V_2 \simeq 1.5\, V_1$, small enough so that errors due to changing scale on the voltmeter would not be introduced and large enough to maintain adequate sensitivity. The same tests as before were applied to confirm that the equipment was functioning correctly.

Some results were obtained by this method at 20 mc/s as well as at 5 mc/s. These and previous results are shown in
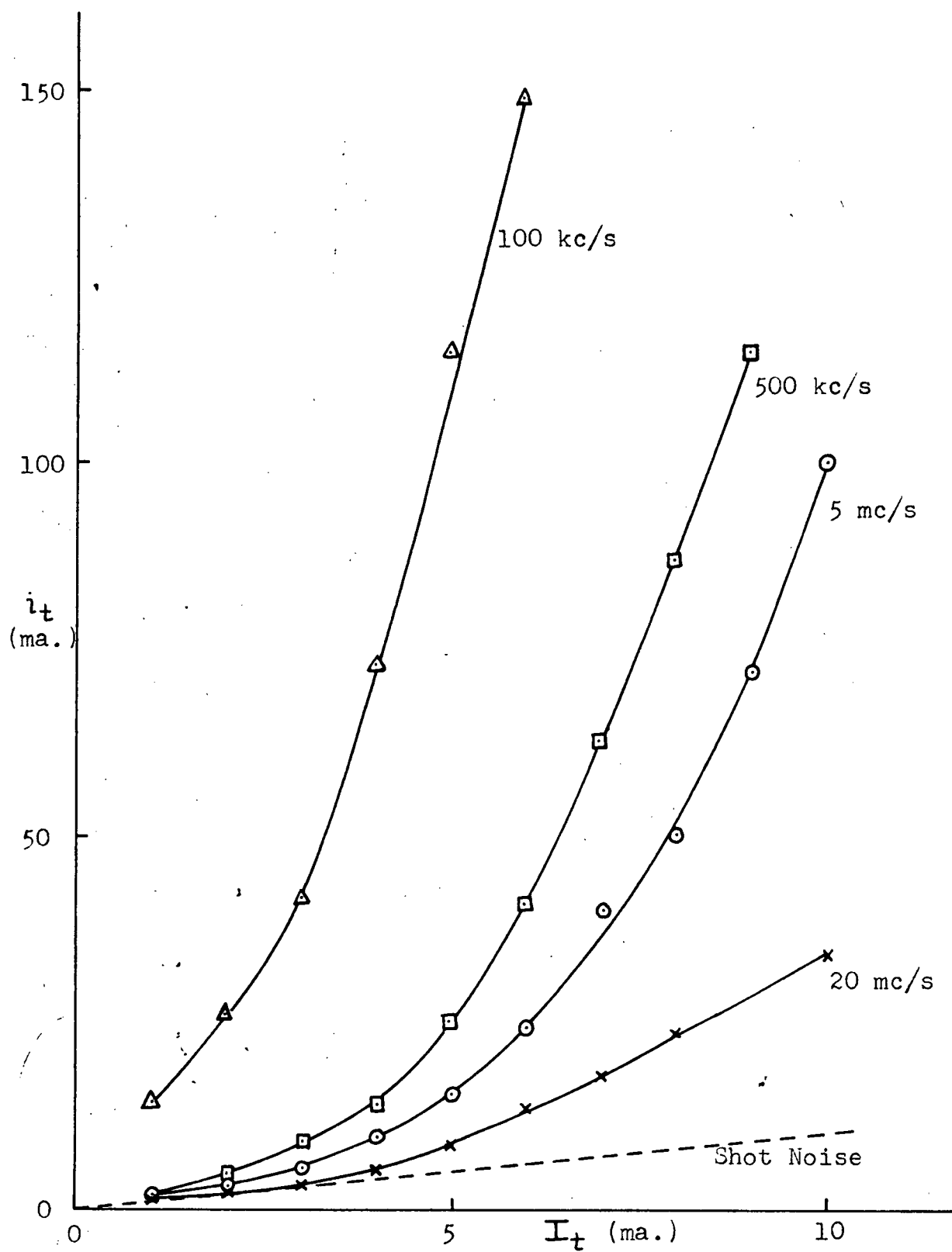
Figure 18 - Variation of Transistor Noise with Current and Frequency for 2N137 #21

figure 18 to give an overall picture of the variation of transistor noise with current and frequency.

The noise currents at 5 mc/s and for small transistor currents were measured and found similar to those shown in figure 20. This graph is interpreted as indicating the absence of excess noise below 1 ma.; it is seen that if shot noise is subtracted that the transistor thermal noise was slightly increasing with current between 0.1 ma. and 1.0 ma., and very rapidly rising at higher currents. The latter was presumed to be caused by the onset of excess noise which was found to be very current-dependent.

It was not possible to make low current measurements at higher frequencies since the amplifier noise increased and overrode the transistor noise. The length of the circuit wiring was also considered excessive for obtaining reliable results above 5 mc/s.

The low current data obtained by this method were rather scattered and to some extent non-reproducible in absolute values; this was attributed to the fact that the circuit was being used close to the limit of its sensitivity and consequently the equipment was modified specifically for the low current measurements.

3.8   Noise Measurements at Low Currents

The sensitivity of the circuit was improved greatly by increasing the noise voltage at the input to the first
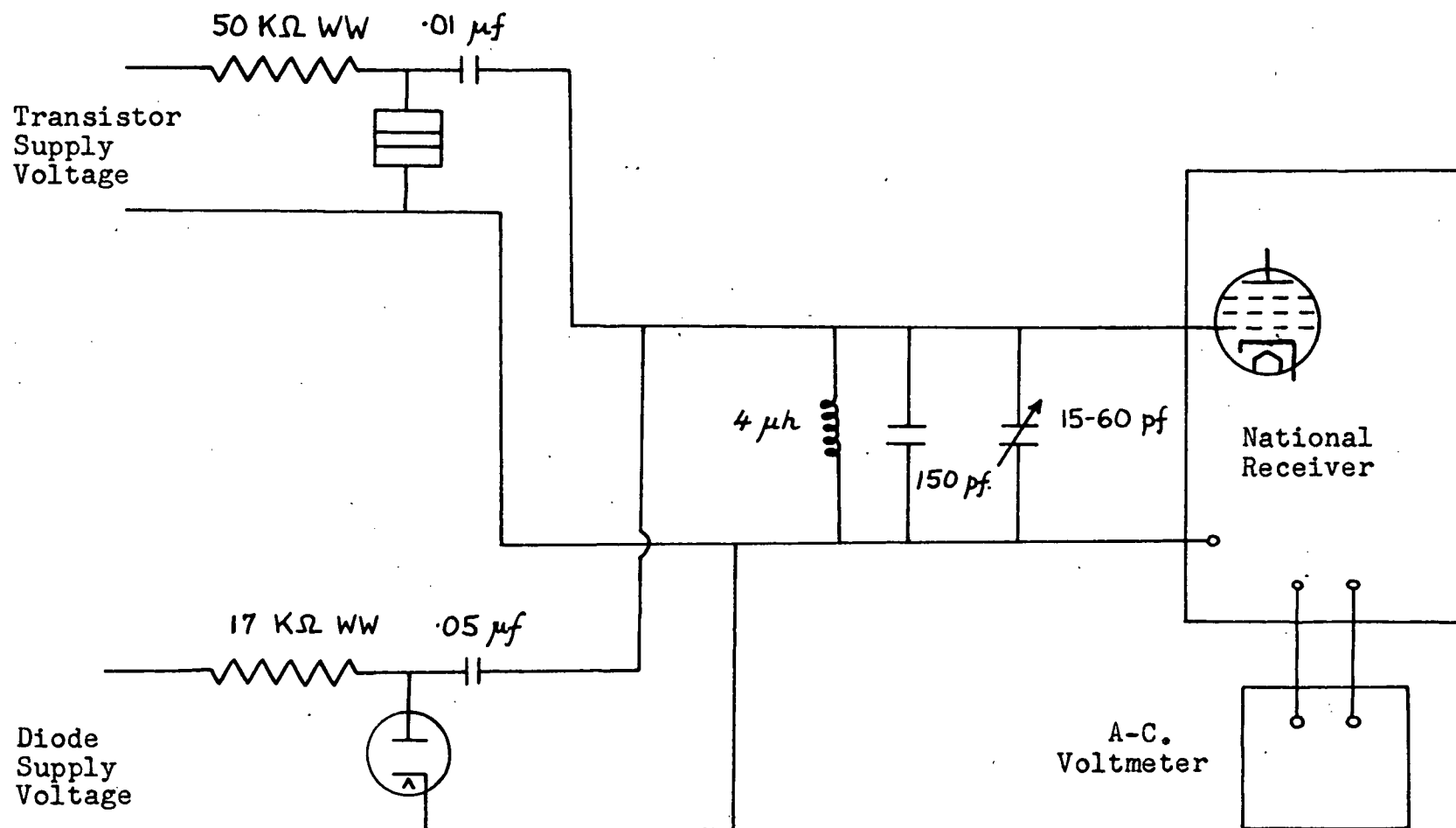
Figure 19 - Circuit for Measurements at Low Currents and at 5 mc/s.

amplifier of the receiver. Since the noise voltage is equal to
the product of the noise current and the modulus of the circuit
impedance, increasing the latter to the maximum possible
gives the most favourable ratio of transistor to amplifier noise.
The circuit admittance was ultimitely limited by the transistor,
and at high currents this condition was achieved previously.
With low currents the transistor R_t was typically 2,000 Ω
and it was obvious that a marked improvement could be made.

The load resistors were increased to 17 KΩ and 50 KΩ for
the diode and transistor respectively. The noise was fed into
a 5 mc/s tuned circuit and thence directly to the grid of the
first tube of a National receiver as shown in figure 19. The
tuned impedance of the whole circuit was measured to be 3500 Ω
on the Wayne Kerr bridge; this low value was attributed to coil
losses due to the close proximity of the chassis, but it was
high enough for the purpose for which the circuit was designed.

The equivalent circuit for this method was the same as
that for the first method of measuring noise shown in figure 15.
In this case R_L= 3.5 K and its thermal noise could no longer
be neglected. The procedure for noise measurement that was
adopted was essentially the same as that described in section
3.7 except that V_0 was measured with the receiver input shorted
and the thermal noise of R_L was subtracted directly giving

$$i_t = I_d \left\{ \frac{V_1^2 - V_0^2}{V_2^2 - V_1^2} \right\} - \frac{4kT_0}{2q} \cdot \frac{1}{R_L} \qquad (3.8.1)$$

As a check, the noise of R_L was measured by this method with
the transistor disconnected, and found to agree within 10% of
the expected value for R_L= 3.5 K . This agreement was as good
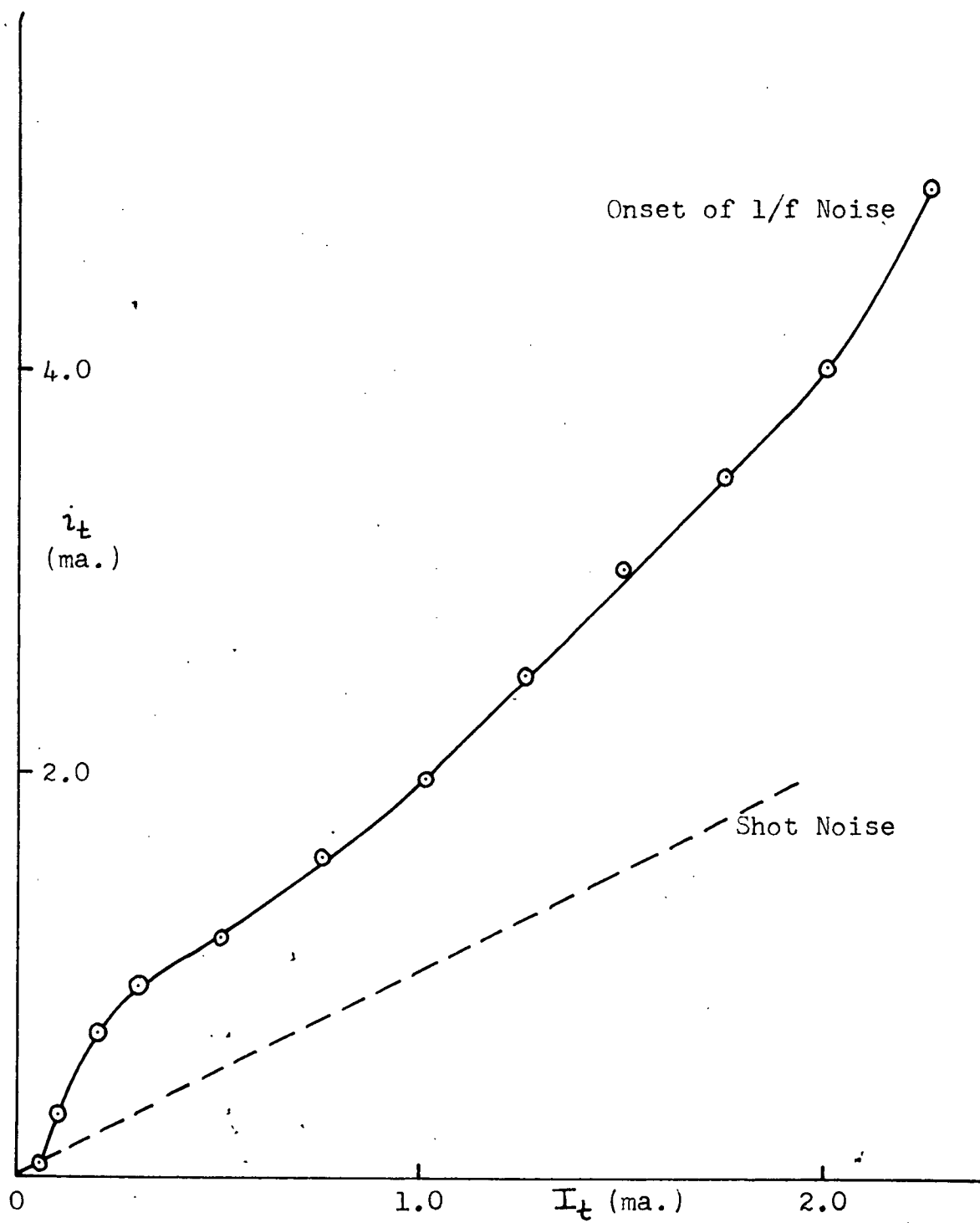
Figure 20 — Variation of Transistor Noise with Current at 5 mc/s for 2N137 #21

as could be expected from the sensitivity of the apparatus, but was not achieved until the Transpac supply to the noise diode filament was replaced by a battery; it was discovered that some external noise was being introduced through the leads from the Transpac.

The linearity of the receiver was tested by determining the variation of the output voltage squared with the diode current as before; this graph was found to be a straight line for the voltages used, but deviated at higher voltages due to the a.v.c. of the receiver. Measurement of the noise of another noise diode gave a maximum error of 0.02 ma. for currents up to 0.15 ma.
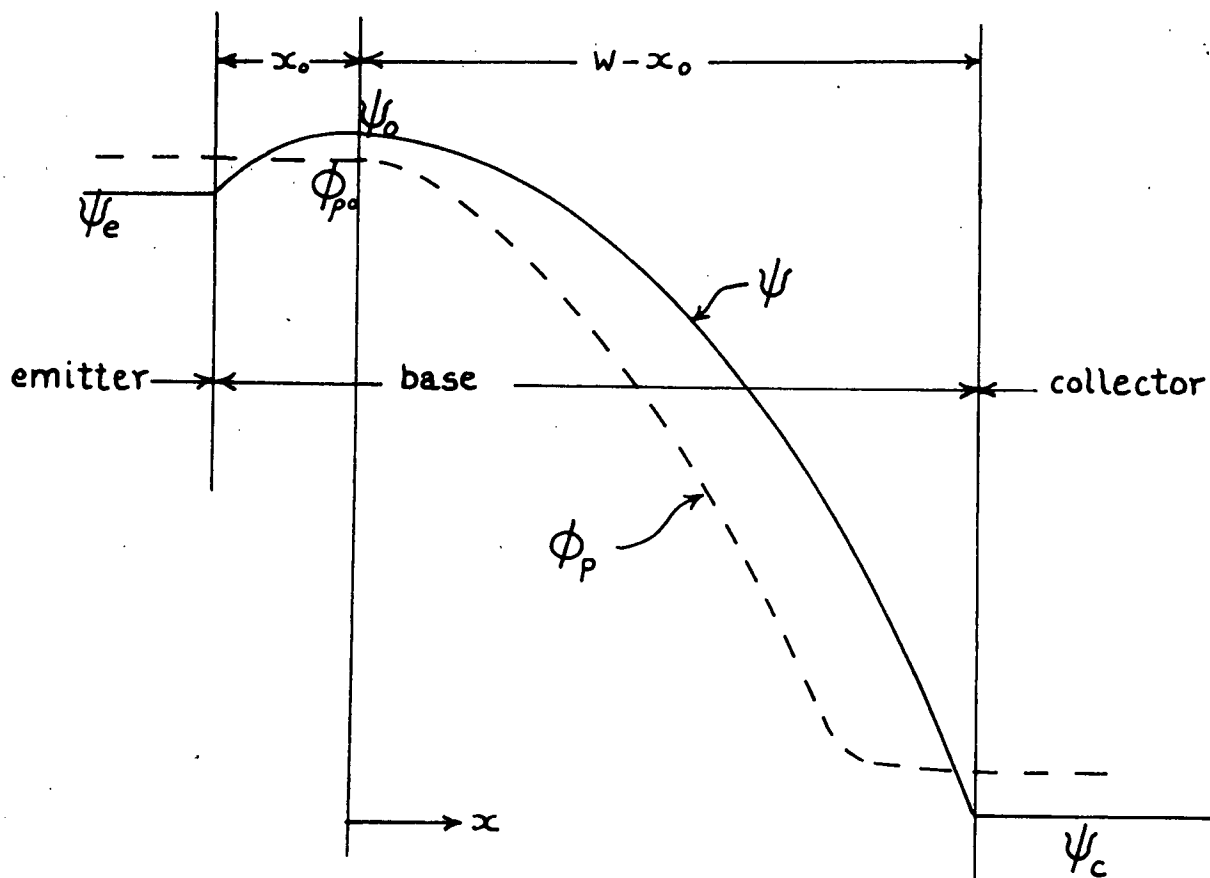
Figure 21 - Electrostatic Potential ψ and quasi Fermi level for Holes ϕ_P in a P-n-p Diode

Chapter IV -- THEORY

4.1   The Punch-through Voltage

The standard equation for the punch-through voltage of a transistor, equation (1.3.1), is obtained by a double integration in one dimension of Poisson's equation over the base width, assuming a uniform charge density due to the donor ions, and using the boundary conditions that the electrostatic potential and the electric field are equal to zero at the emitter junction. However, there is a potential rise in front of the emitter which, though small, is not negligible in transistors with a low punch-through voltage.

The electrostatic potential ψ and the quasi Fermi level for holes φ_p shown in figure 21 are defined as follows. ψ is the energy midway between the valence and conduction bands of the material such that in intrinsic material it is equal to the Fermi level energy. The quasi Fermi level φ_p for holes is defined by the equation

$$p = n_i \exp \left\{ \frac{q(\varphi_p - \psi)}{kT} \right\} \qquad (4.1.1)$$

and similarly the quasi Fermi level φ_n for electrons is defined by

$$n = n_i \exp \left\{ \frac{q(\psi - \varphi_n)}{kT} \right\} \qquad (4.1.2)$$

where p is the hole density, n the electron density, and $n_i = p = n$ in intrinsic material. It is seen that for p-type

material where $p > n$, that $\phi_p > \psi$ and $\phi_n < \psi$; the converse is true for n-type material. Substituting equation (4.1.1) into the equation for the hole current due to drift and diffusion yields

$$J_p = -q D \nabla p - q \mu p \nabla \psi = q \mu p \nabla \phi_p \qquad (4.1.3)$$

where D and μ are the hole diffusivity and mobility respectively. A similar equation exists for the electron current.

We shall now justify the variation of ϕ_p and ψ shown in figure 21 and then derive an expression for the height of the potential maximum in front of the emitter in terms of the current. In the emitter and collector regions, the hole density is about 10^{18} to 10^{19} cm^{-3}, very much higher than n_i which is 3.10^{13} for germanium, thus $\phi_p > \psi$; also for small current densities, since p is so large, a good approximation is $\nabla \phi_p = \nabla \psi = 0$. In the base region for $x > 0$, the current is predominantly a drift current and for $p = \frac{J}{q \mu \nabla \psi} \ll N$ the donor density in the base, the potential distribution can be calculated using Poisson's equation

$$\nabla^2 \psi = -\frac{q N}{\epsilon} \qquad (4.1.4)$$

Imposing the boundary conditions that $\psi = \nabla \psi = 0$ at $x = 0$, assuming that N is independent of x, and assuming planar geometry gives

$$\psi = -\frac{q N}{2\epsilon} x^2 \qquad \text{for} \qquad 0 < x < (W - x_0) \qquad (4.1.5)$$

Since p decreases with x in this region, the difference $\psi - \phi_p$ must increase according to equation (4.1.1). At the collector junction, because of the sudden increase of p, both $\nabla \psi$ and $\nabla \phi_p$

decrease very sharply and ψ and φ_p take on their equilibrium values in the material.

That there exists a potential maximum in front of the emitter is seen to be necessary to limit the current flowing through the diode. In the region $x<0$, a good approximation is that φ_p is a constant because the high hole density of the emitter spreads into the base for a few free mean free paths. The hole density at $x=0$ can be calculated from (4.1.1) with φ_p and ψ evaluated at $x=0$.

$$p(0) = n_i \exp\left\{-\frac{q}{kT}(\varphi_{P_0}-\psi_0)\right\} \tag{4.1.6}$$

If we consider that any hole travelling in the $+x$ direction at $x=0$ is immediately grabbed by the field and shot off to the collector, the current can be calculated from the mean velocity of the holes in the $+x$ direction at this point. Assuming that the holes have a Maxwellian velocity distribution, the current density is

$$J = q\left(\frac{kT}{2\pi m}\right)^{1/2} n_i \exp\left\{\frac{q(\varphi_{P_0}-\psi)}{kT}\right\} \tag{4.1.7}$$

The difference between ψ_e and φ_{pe} in the emitter can be calculated from (4.1.1) if the emitter impurity density p_e is known,

$$p_e = n_i \exp\left\{\frac{q(\varphi_{pe}-\psi_e)}{kT}\right\} \tag{4.1.8}$$

Combining (4.1.7) and (4.1.8) gives for the height of the potential maximum, assuming that $\varphi_{pe} = \varphi_{P_0}$,

$$\psi_0 - \psi_e = \frac{kT}{q} \ln\left\{\frac{q p_e}{n}\left(\frac{kT}{2\pi m}\right)^{1/2}\right\} \tag{4.1.9}$$

The assumption that for $x < 0$, ϕ_p is a constant can now be checked; the value of $\nabla \phi_p$ at $x = 0$ can be calculated from equations (4.1.3), (4.1.6) and (4.1.7). This yields

$$\nabla \phi_p (x=0) = \left(\frac{kT}{2\pi m}\right)^{1/2} \cdot \frac{1}{\mu} \qquad (4.1.10)$$

Substituting the values $\mu = 1900$ cm²/volt sec., $m = 0.4$ x the free electron mass (Conwell, 1958) and $T = 300°K$ gives $\nabla \phi_p = 2,000$ volts/cm. If in the base region for $x < 0$, the average value of $\nabla \phi_p$ is only half this value, for $x_0 = 10^{-5}$cm., the change in ϕ_p, $\phi_{pe} - \phi_{p_0} \approx 0.01$ volt.

Since the reading of a voltmeter across the emitter-collector diode will be equal to the difference of the quasi Fermi levels in the two p regions, the measured punch-through voltage will be,

$$V_p = \frac{qN}{2\epsilon} W^2 - \frac{kT}{q} \ln \left\{ \frac{q P_e}{n} \left(\frac{kT}{2\pi m} \right)^{1/2} \right\} \qquad (4.1.11)$$

assuming that the two p regions are similar, that is that

$$\phi_{pe} - \psi_e = \phi_{pc} - \psi_c .$$

A further deviation from the usual formula for the punch-through voltage can occur if the collector surface is not planar; in particular if it is spherical, and if it is also assumed that the emitter surface is spherical concentric with the collector surface, the new punch-through voltage obtained from the double integration of Poisson's equation in spherical geometry is

$$V_p = \frac{qN}{2\epsilon} W^2 \left\{ 1 + \frac{W}{3 r_c} \right\} - \frac{kT}{q} \ln \left\{ \frac{q P_e}{n} \left(\frac{kT}{2\pi m} \right)^{1/2} \right\} \qquad (4.1.12)$$

where r_c is the radius of curvature of the collector surface.

4.2   Noise in a Specimen with Non-uniform Field

In Appendix II it is shown that the noise in a specimen with a uniform field distribution is equal to the sum of shot and thermal noise; to find the noise in a specimen with non-uniform field distribution we shall consider the noise voltage $\overline{\Delta v^2}$ generated by a section of thickness Δx in which the field may be considered uniform and then consider the specimen as a series of noise voltage generators. At this point it is necessary to be very careful in evaluating the total specimen noise voltage.

For frequencies much less than the reciprocal of the transit time, the shot noise component of all sections is completely correlated and it may be represented by a noise current generator of value $S_i(f) = 2q I$ in parallel with the specimen. The shot noise is independent of the field distribution for frequencies much less than the reciprocal of the transit time since the current consists of a series of spikes, the Fourier analysis of which does not depend on their shape, but on the total area q of each spike and the mean current.

In evaluating the thermal noise, the section thickness must be chosen large enough so that the noise voltages of neighboring sections is uncorrelated, in which case the $\overline{\Delta v^2}$ can be summed; this means that several collisions should take place in Δx for each carrier. Δx must also be chosen small enough so that the field may be considered constant within Δx.

Under these conditions the total thermal noise voltage of the specimen is equal to

$$\overline{U^2} = \sum_{j} \overline{\Delta u_j^2}$$ (4.2.1)

For each section Δx we may also define an a-c. resistance ΔR and an effective carrier noise temperature T_n which is in general a function of the electric field F. The total a-c. resistance of the specimen is given by $R_0 = \sum_{j} \Delta R_j$ where it has been assumed that imaginary admittance components are negligible. The spectral density of the thermal noise is then given by

$$S_v(f)_{th} = 4k \sum_{j} T(F) \Delta R_j$$ (4.2.2)

This may now be converted to an integral over the variable x, which represents the distance across the specimen in the direction of the field.

$$S_v(f)_{th} = 4k \int T(x) \frac{dR}{dx} dx$$ (4.2.3)

To evaluate the integral it is necessary to know both the field distribution in the specimen and the dependence of the carrier noise temperature on the field. The reason that (4.2.1) cannot be integrated and that (4.2.2) can is that ΔR_j takes into account the correlation between the noise voltages in neighboring sections.

4.3 . Noise Temperatures

In a vacuum diode there is shot noise due to the random emission of electrons, but no thermal noise; however, the

electrons have a high mean kinetic energy. It is obvious then that Shockley's definition of the effective temperature as $(1/k) \times$ (mean kinetic energy) cannot be used as the noise temperature, which is zero in the above example. For the particular case of a solid in which the drift velocity is independent of the spatial coordinates, it is shown in Appendix II that the temperature to be used in considering thermal noise is given by

$$k T_n = m \left(\overline{u^2} - \overline{u}^2 \right) = m \cdot var\, u \qquad (4.3.1)$$

where u is the velocity in the direction of the field and T_n is the noise temperature.

To apply this to the theory of Yamashita and Watanabe (1954) discussed in section 2.4, it is necessary to make an assumption about the velocity distribution and then find the velocity variance in terms of the mean energy and drift velocity. A logical and simple distribution is an isotropic one displaced by the drift velocity $\overline{u}$. Let us denote the velocity components in three mutually orthogonal directions by v_x, v_y and v_z, where v_x and u are in the same direction. The mean electron energy is then

$$\overline{E} = \frac{1}{2} m \left(\overline{v_x^2} + \overline{v_y^2} + \overline{v_z^2} \right) \qquad (4.3.2)$$

but accoring to the assumption made about the velocity distribution we also have

$$\overline{v_y^2} = \overline{v_z^2} = \overline{(v_x - \overline{u})^2} = \overline{v_x^2} - \overline{u}^2 \qquad (4.3.3)$$

Combining the last three equations and noting that u and v_x are

equivalent quantities yields the required formula for the noise temperature

$$kT_n = \frac{2}{3}\overline{E} - \frac{1}{3}m\overline{u}^2 \qquad (4.3.4)$$

Since the maximum possible value of $\overline{u}$ is 7.10^6 cm/sec. for holes in germanium from the experiments of Ryder (1953) and Larrabee (1959), and the minimum possible value of $\overline{E}$ is $\frac{3}{2}kT_0$, the maximum value of the ratio of the second to the first term of (4.3.4) is

$$\left(\frac{m\overline{u}^2}{2\overline{E}}\right)_{max} = 0.12 \qquad (4.3.5)$$

where $m = \frac{1}{3}$ (free electron mass) has been used. The theory of Shockley indicates however that at this high velocity, $\overline{E}$ will be much greater, and using the results of equations (2.3.4) gives instead for the maximum value

$$\left(\frac{m\overline{u}^2}{2\overline{E}}\right)_{max} = 0.03 \qquad (4.3.6)$$

Consequently we are justified in neglecting the second term in equation (4.3.4). The same result does not hold true for electrons because of their much higher effective mass (see Conwell, 1958).

On this basis then it is deduced that Shockley's equations (2.3.4) for effective hole temperatures can be used in good approximation for the noise temperatures. It is interesting in this connection to calculate the mean energy and noise temperature of the distribution (2.4.1) derived by Yamashita and Watanabe (1954). Making the substitution $x = \frac{E}{kT_0}$, the mean energy is given by
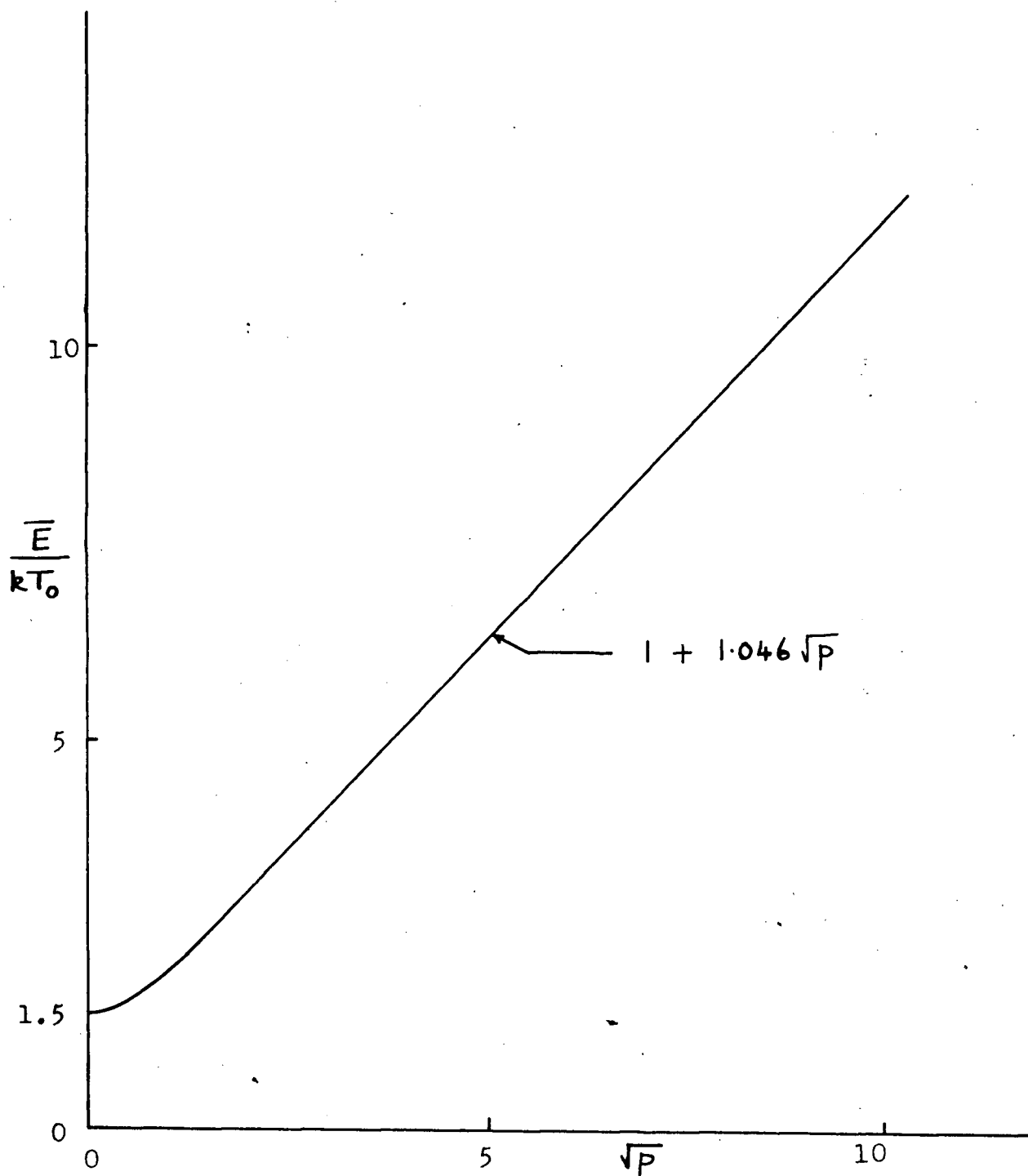
Figure 22 – Mean Energy $\overline{E}$ as a Function of $\sqrt{P}$, a parameter proportional to the Electric Field, for the Pisarenko Distribution

$$\overline{E} = kT_0 \frac{\int_0^\infty x^{3/2} (x+p)^P e^{-x} dx}{\int_0^\infty x^{1/2} (x+p)^P e^{-x} dx} \qquad (4.3.7)$$

where p is a parameter proportional to the square of the field and is given more explicitly in scetion 2.4. For integral values of p this can be evaluated by expanding the bracketed terms and evaluating the resulting series of gamma functions. this is only convenient for small values of p, but for $p \gg 100$ the approximation $x \ll p$ can be made over the range of integration and (4.3.7) becomes

$$\overline{E} = kT_0 \frac{\int_0^\infty x^{3/2} e^{-\frac{x^2}{2p}} dx}{\int_0^\infty x^{1/2} e^{-\frac{x^2}{2p}} dx} \qquad (4.3.8)$$

This can easily be evaluated in terms of gamma functions to give

$$\overline{E} = 1.046 \sqrt{p} \, kT_0 \qquad p \gg 100 \qquad (4.3.9)$$

Graphical integration methods were used for the evaluation of the integrals at $p = 100$. The results for the mean energy are shown in figure 22 and an excellent approximation to the curve is

$$\overline{E} = \left\{ 1 + 1.046 \sqrt{p} + 0.5 \, e^{-2.092 \sqrt{p}} \right\} kT_0 \qquad (4.3.10)$$

It is possible to evaluate the proportionality constant between p and F^2 in terms of the zero field mobility which is given by Yamashita and Watanabe as $\mu_0 = 4q\ell /3\sqrt{2\pi m kT_0}$. This gives for p

$$\sqrt{p} = \frac{q \ell F}{s \sqrt{6mkT_0}} = \frac{\sqrt{3\pi}}{4} \frac{\mu_0 F}{s} = \sqrt{2} \frac{F}{F_0}$$

where $F_o = \frac{S}{\mu_o}\sqrt{\frac{32}{3\pi}}$ has been substituted. Substituting for p in equation (4.3.10) and noting that the second term in (4.3.4) is negligible as shown previously, we have for the noise temperature

$$T_n = T_o \left\{ \frac{2}{3} + \frac{F}{F_o} + \frac{1}{3} \exp\left(-\frac{3F}{F_o}\right) \right\} \qquad (4.3.11)$$

This is almost identical to the results obtained by Shockley, equations (2.3.4).

We shall now calculate the noise temperature to be expected on the basis of Gunn's model discussed in section 2.4. Substituting the values for the drift velocity and mean square velocity from (2.4.2) into equation (4.3.1) yields

$$T_n = \frac{1}{6} T_{op} = 85\,^{\circ}K \qquad (4.3.12)$$

Though this method of calculating the noise temperature on the basis of Gunn's model is not completely valid, because the postulated carrier motion does not follow the statistics assumed in deriving equation (4.3.1), the overall result that the noise temperature is much less than $(1/k)$x(mean kinetic energy) still holds. Such a temperature is quite impossible for a lattice at room temperature, and consequently from the point of view of the noise temperature it is seen that Gunn's model is quite inadequate. It may be said in general then that though a test of a model be that it predicts the correct velocity-field relation, an even more stringent test is that it predicts reasonable values for the velocity fluctuations.
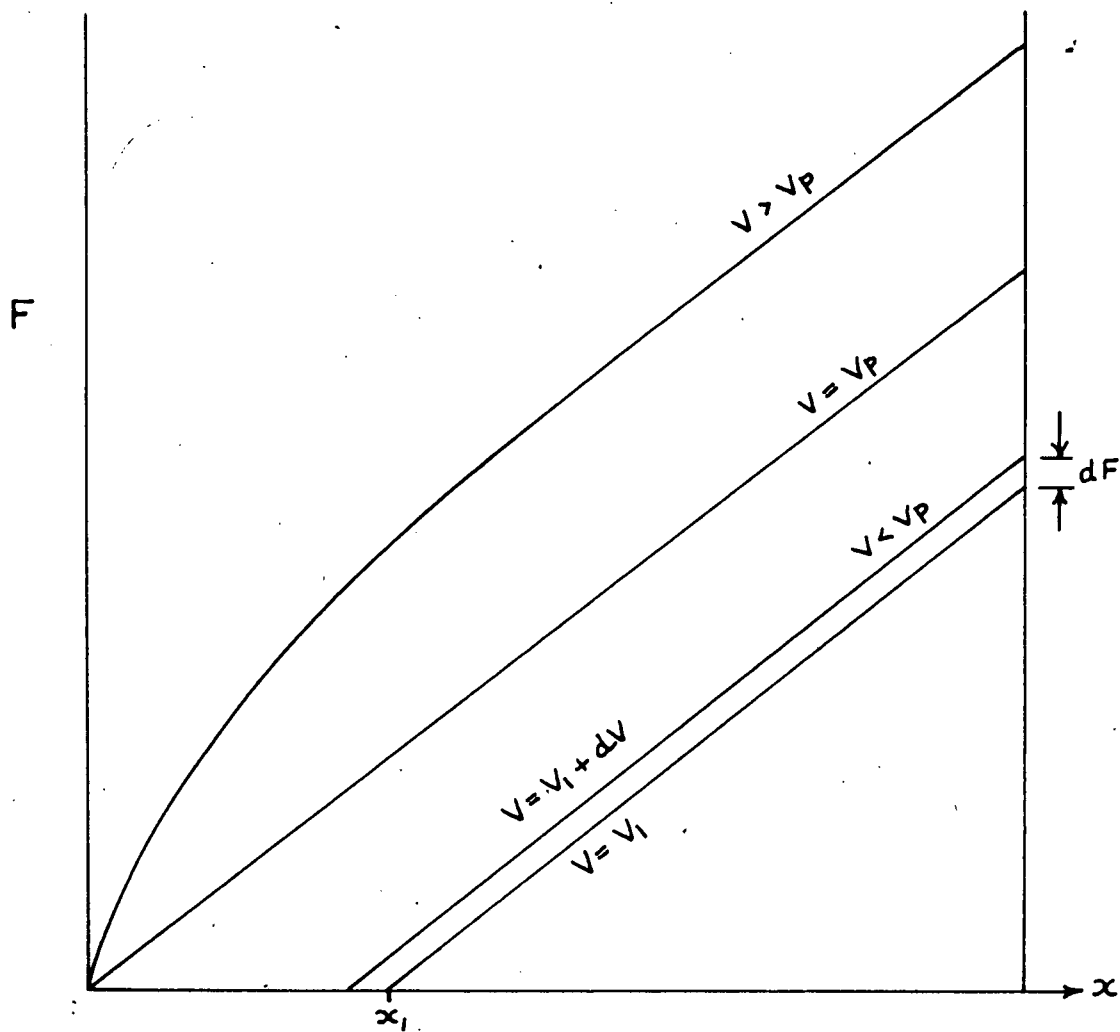
Figure 23 — Field Distribution in the Base for Various Applied Voltages

4.4 Thermal Noise of a P-n-p Diode

In evaluating the thermal noise of a p-n-p diode we first assume that all the applied voltage and changes thereof appear across the space-charge-limited region of the base; then, if the electric field distribution across the base, and the dependence of the carrier noise temperature on the field are known, equation (4.2.3) can be used to evaluate the thermal noise. The electric field distribution across the base is shown in figure 23 for several typical operating conditions of the diode, and it is obvious that the regions $V < V_P$ and $V > V_P$ must be discussed separately.

For the region $V < V_P$, the field distribution can be found from integrating Poisson's equation $\nabla F = \frac{\rho}{\epsilon}$, where ρ is the donor charge density of the base, and using the boundary condition that $-\int_{x_1}^{W} F\, dx = V$ the applied voltage, where x_1 is the boundary of the space-charge region. The field is thus found to be

$$F = \frac{\rho}{\epsilon}(x - x_1) \quad , \quad x_1 = W - \sqrt{\frac{2\epsilon V}{\rho}} \qquad x_1 < x < W. \qquad (4.4.1)$$

Substituting the formula $V_P = \frac{\rho}{2\epsilon} W^2$ for the punch-through voltage yields

$$F = \frac{2V_P}{W^2}(x - x_1) \quad , \quad x_1 = W\left(1 - \sqrt{\frac{V}{V_P}}\right) \qquad x_1 < x < W. \qquad (4.4.2)$$

The incremental resistance at any point is then given by

$$dR = \left(\frac{dF}{dI}\right) dx = \left(\frac{dF}{dV}\right)\left(\frac{dV}{dI}\right) dx. \qquad (4.4.3)$$

Substituting $\frac{dF}{dV}$ from (4.4.2) and noting that $\frac{dV}{dI} = R_0$, the

overall resistance of the specimen, yields

$$dR = \frac{1}{W} \sqrt{\frac{V_P}{V}} \, R_0 \, dx. \qquad (4.4.4)$$

Substituting the formulae (4.4.2) for the field distribution, (4.4.4) for the incremental resistance, and (4.3.11) for the noise temperature into equation (4.2.3) yields for the spectral distribution of the noise voltage

$$S_V(f) = 4kT_0R_0\left\{ \xi + \frac{2}{3} + \frac{1}{18\xi}\left(1 - \exp(-6\xi)\right)\right\} \qquad (4.4.5)$$

where

$$\xi = \frac{\sqrt{VV_P}}{WF_0}.$$

Defining an average temperature T' by $S_V(f) = 4kR_0T'$, we find for the limiting values

$$\sqrt{VV_P} \ll WF_0 \qquad T' = \left(1 + \frac{2VV_P}{W^2F_0^2}\right)T_0$$

$$\sqrt{VV_P} \gg WF_0 \qquad T' = \frac{\sqrt{VV_P}}{WF_0}\,T_0 \qquad (4.4.6)$$

For $V > V_P$ it is convenient to use the field distribution (2.2.5) derived by Nichol for small current densities. In this case

$$dR = \frac{3}{2}R_0\,W^{-\frac{3}{2}}\sqrt{x}\,dx \qquad (4.4.7)$$

It is convenient mathematically to discuss the average temperature T' for two approximations. In the case that the field $F \ll F_0$ throughout the base, the noise temperature can be approximated by $T_n = T_0\left(1 + \frac{3}{2}\frac{F^2}{F_0^2}\right)$ and the average temperature is then given by

$$\frac{T'}{T_0} = 1 + \frac{9}{4}\left\{\sqrt{\frac{8}{7}}\frac{V_P}{WF_0} + \frac{3}{2\sqrt{5}}\frac{C}{F_0 W}(V-V_P)\right\}^2. \qquad (4.4.8)$$

In the case that the approximation $F \gg F_0$ throughout most of the base can be made, $T_n = T_0\left(\frac{2}{3} + \frac{F}{F_0}\right)$ and

$$\frac{T'}{T_0} = \frac{2}{3} + \frac{6}{5}\frac{V_P}{N F_0} + \frac{9C(V-V_P)}{8\sqrt{2}F_0 W}. \qquad (4.4.9)$$
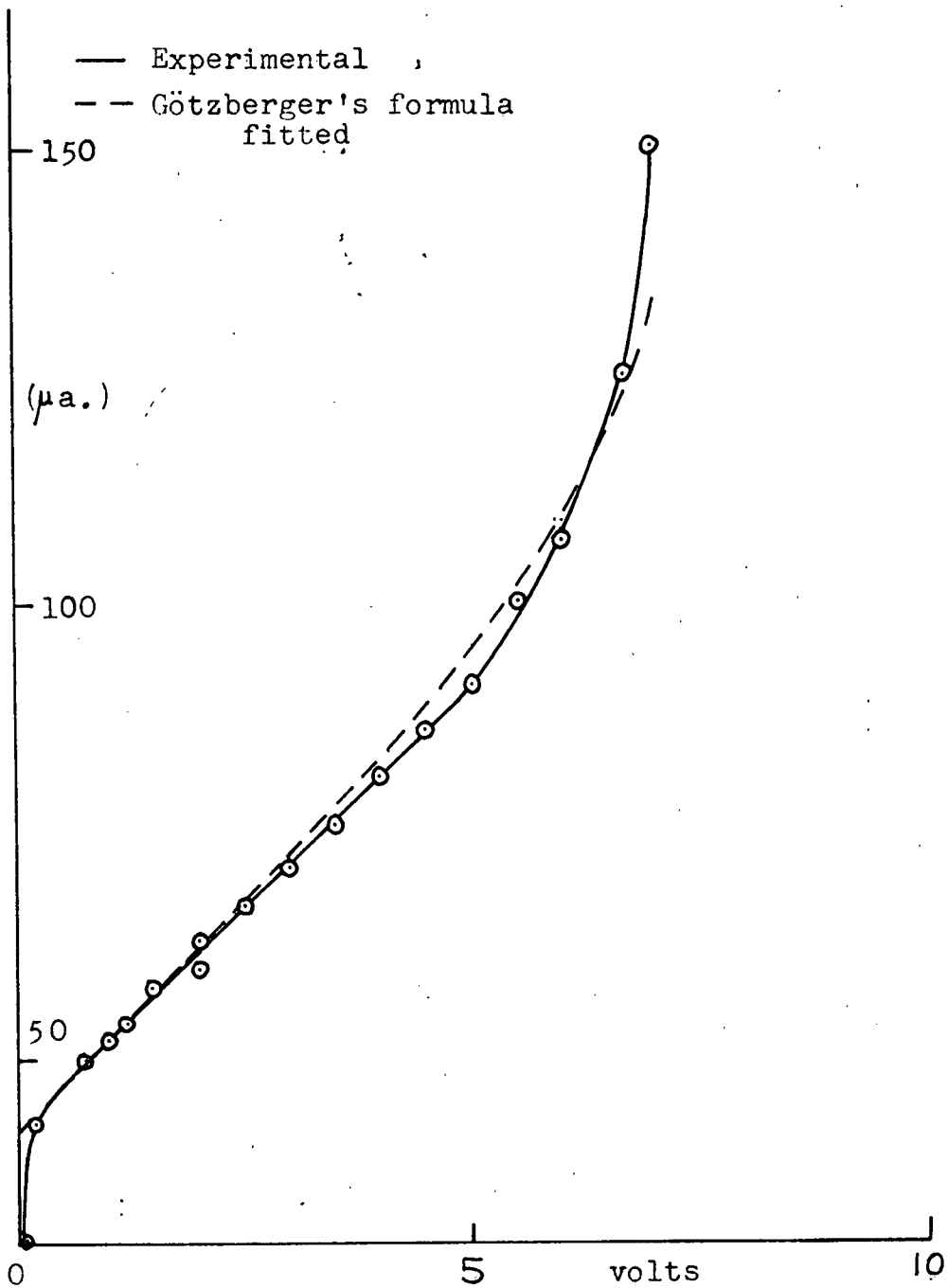
Figure 24 - Götzberger's Formula fitted to the D-C. Current-Voltage Characteristic of 2N137 #21

Chapter V -- DISCUSSION OF RESULTS

5.1   D-C. Characteristics

The d-c. current-voltage characteristics of a typical p-n-p diode are shown in figure 7. Theoretical considerations of the two voltage ranges, below and above the punch-through voltage, were discussed in sections 2.1 and 2.2 respectively and the agreement is good except for the constant in Nichol's equation (2.2.8).

Götzberger's equation (2.1.4) was fitted to the experimental results for the pre-punch-through voltages and the comparison is shown graphically in figure 24. The numerical values for the curve shown are

$$I = \frac{42}{1-\sqrt{\frac{V}{17\cdot5}}} + \frac{1\cdot3}{1-\sqrt{\frac{V}{7\cdot5}}} \qquad \text{for } V < 7 \text{ volts} \qquad (5.1.1)$$

where the current I is in microamperes and the voltage is in volts. The measured value of $I_{co} = 0.5 \pm 0.05$ μamps. was not observed to change over the voltage range considered so it was not necessary to make any correction for this.

In Götzberger's model, equation (5.1.1) represents two transistors in parallel with punch-through voltages of 7.5 and 17.5 volts respectively, and relative areas of 1.3 : 42. The ratio of the two base widths can be calculated from the two punch-through voltages and is 1 : 1.5. It should be noted that the low V_p of 7 volts is higher by 1 volt than the measured

Schenkel-Statz punch-through voltage. Nichol found it necessary to assume spherical geometry for the collector junction and the space-charge region to explain the post-punch-through current; this is quite consistent with the above results and the latter indicate that the maximum base width is at least 1.5 times the minimum. The two punch-through voltages do not indicate extreme values, but intermediate values which give the best approximation to Götzberger's model.

The post-punch-through current was observed experimentally to be

$$I = 2.4 \cdot 10^{-5} (V-V_p)^3 \qquad (5.1.2)$$

where V and V_p are in volts and I is in amperes. This is in qualitative agreement with Nichol's equation (2.2.4), however substituting the appropriate vale of $\mu_o = 1900$ cm^2/volt.sec. (Conwell, 1958) and $W = 1.3 \cdot 10^{-3}$ cm. deduced from the manufacturer's value of the cutoff frequency $f_\alpha = 8$ mc/s into the equation gives $I = 1.2 \cdot 10^{-6} (V-V_p)^3$. This numerical discrepancy can be explained in terms of the effective emitter area that Nichol uses; he considers this to be the area of the emitter plane intersected by a spherical space-charge region with centre at the collector junction. The assumption of a zero collector radius is not valid and even so Nichol does not use the correct form for the punch-through voltage in spherical geometry. If the collector junction is assumed to be spherical with radius λ_c, then using spherical geometry, and assuming that $3\lambda_c \gg W$, the effective emitter area A_e is

$$A_e = \frac{\pi \lambda_c W}{V_p} (V - V_p) \qquad \text{for} \quad V > V_p \qquad (5.1.3)$$

which is larger than Nichol's by a ratio of $\frac{\lambda_c}{W}$; the current would be expected to be larger by the same ratio. From the above correction, it is possible to deduce a value of the collector radius $\lambda_c = 20W = 2.6 \cdot 10^{-2}$cm. for the transistor G.E. 2N137 #21. This value justifies the approximation that $3\lambda_c \gg W$ made in deriving equation (5.1.3).

5.2   A-C. Characteristics

The experimental results are shown in figure 10,11,12 and 13, and can be explained by means of the following model. The transistor diode is considered to consist of a resistance R_0 in series with an admittance $Y(f)$; R_0 represents the resistance of the base region in which the drift current predominates, while $Y(f)$ represents the admittance of the base region in which the diffusion current predominates, that is in the vicinity of the potential maximum. Shockley (1949) gives for the diffusion admittance of a p-n junction

$$Y(f) = G_o \left(1 + j\omega T \right)^{1/2} \qquad (5.2.1)$$

where

$$G_o = \frac{q P_n \mu A}{L_p} \exp \left(\frac{q V_o}{kT} \right) \qquad (5.2.2)$$

The quantities q, V_o, T, P_n and L_p have been defined with equation (1.2.2), and T is the lifetime of a hole in the n region; μ is the hole mobility in the n region. This equation

is derived in a similar manner to the d-c. equation (1.2.1), but applying an a-c. signal and considering the effects of recombination and generation of the current carriers.

To compare this model with the measured quantities it is necessary to transform the series network into effective R and C components in parallel. Performing this analysis gives

$$R(f) = \frac{1 + 2 R_0 G_0 \theta + R_0^2 G_0^2 (2\theta^2 - 1)}{G_0 \{ \theta + R_0 G_0 (2\theta^2 - 1) \}} \qquad (5.2.3)$$

$$C(f) = \frac{G_0 (\theta^2 - 1)^{1/2}}{\omega \{ 1 + 2 R_0 G_0 \theta + R_0^2 G_0^2 (2\theta^2 - 1) \}} \qquad (5.2.4)$$

where

$$\theta = \frac{1 + (1 + \omega^2 \tau^2)^{1/2}}{2} \, .$$

At high and low frequencies these expression reduce to

$$\omega \tau \gg 1 \qquad R(f) = R_0 \qquad C(f) = \frac{1}{\sqrt{2} R_0^2 G_0 \omega^{3/2} \tau^{1/2}} \quad , \quad (5.2.5)$$

$$\omega \tau \ll 1 \qquad R(f) = R_0 + \frac{1}{G_0} \qquad C(f) = \frac{G_0 \tau}{2(1 + R_0 G_0)^2} \, . \quad (5.2.6)$$

These are in good agreement with the results and in particular agree with the qualitative results of $C \propto f^{-3/2}$ at high frequencies, C constant at low frequencies and a rise of R at low frequencies.

Equations (5.2.5) and (5.2.6) can be considered as four equations in three unknown constants G_0, R_0 and τ. The results are consistent with these four equations, and typical values of the constants are $G_0 = 0.01$ mhos, $R_0 = 350 \, \Omega$ and $\tau = 7 \, . \, 10^{-6}$

secs. for the transistor G.E. 2N137 #53 at a current of 3.0 ma.

An estimate of G_0 can be made from equation (5.2.2) by substituting $\mu = 1900$ cm²/volt sec., $L_p = \sqrt{D T_p}$, $D = \frac{kT}{q}\mu$, $p_n = \frac{n_i^2}{n_n}$,where n_i is the carrier density in intrinsic germanium, and the donor density of the base $n_n = 6 . 10^{13}$ cm⁻³ A is calculated from equation (5.1.3) and V_0 is assumed to be 0.080 volts from the measured floating base potential; this yields a value of $G_0 = .0025$ mhos in fair agreement with the measured value of 0.01 mhos. The most likely source of error is in the value of n_n used, deduced from the measured V_p and assuming a value of W determined from the manufacturer's value of f_α .

5.3   Noise Temperatures

The experimental data of noise current $2q\,i_t$, shown in figure 20, can be transferred into effective hole temperatures T' by first subtracting shot noise $2qI$ and then dividing by $2kG/q$ where G is the measured diode conductance. That this method is valid is concluded from Appendix II where it is shown that shot and thermal noise components are additive; the assumption regarding the transit time can now be checked by calculating it. Assuming that the velocity field relation throughout the base is given by $v = \mu_0\sqrt{F F_0}$ and that the field in the base is $F = \frac{2V_p}{W^2}x$ the transit time is

$$ t_0 = \int_0^W \frac{dx}{v} = \frac{\sqrt{2}\ W^{3/2}}{\mu_0\sqrt{F_0\,V_p}} = 5 \cdot 10^{-10} \text{ secs.} \quad (5.3.1) $$

An estimate of T_0 can be made from the zero field mobility μ_0 which theoretically is equal to $\mu_0 = \frac{q T_0}{m}$. Using a value of

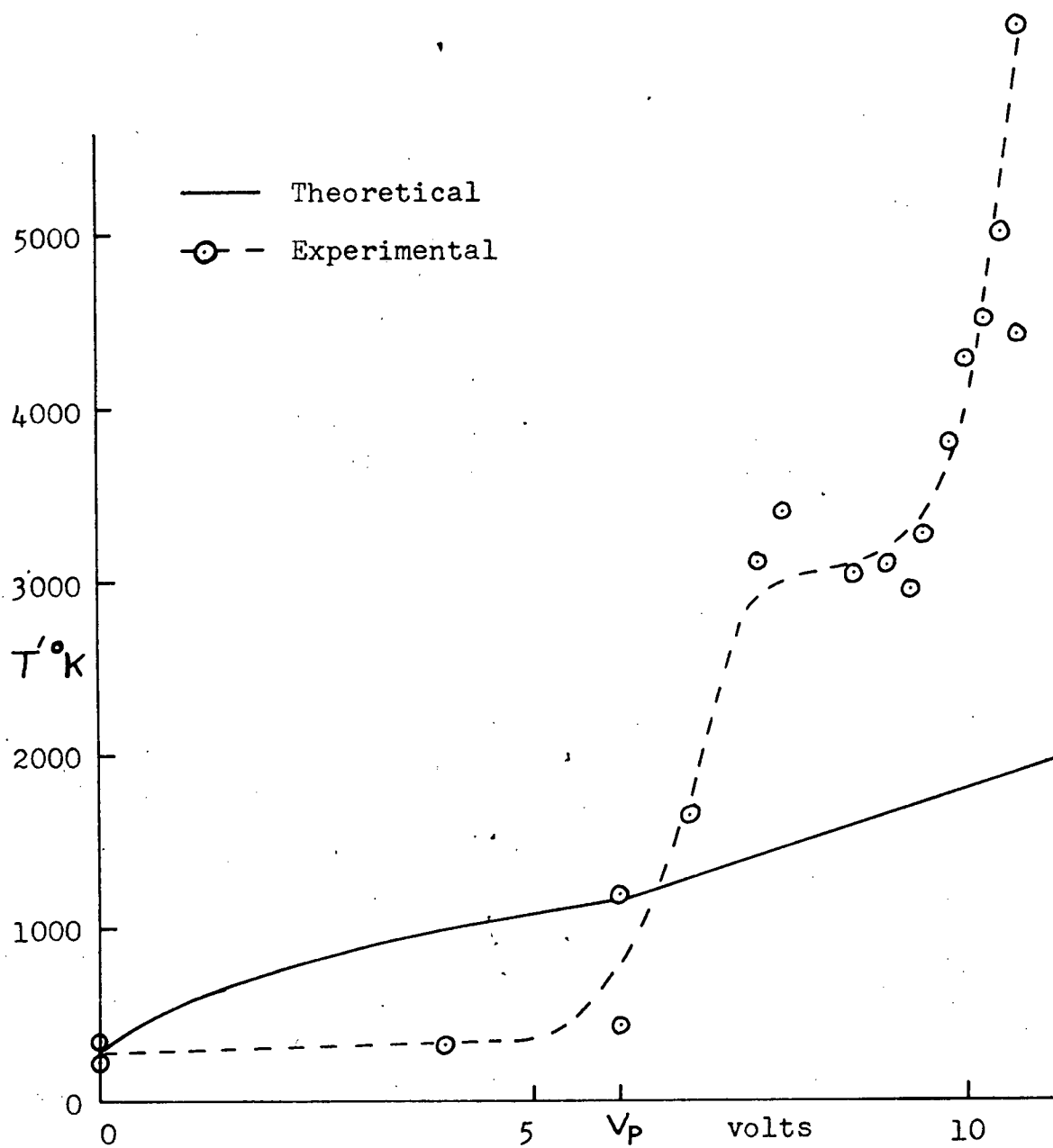**Figure 25** – Comparison of Theoretical and Experimental Values for the Average Hole Temperature T'

$m = (1/3) \times$ (free electron mass) gives $\tau_o = 3.10^{-13}$ secs. and thus the assumption that $t_o \ll \tau_o$ is justified. At the frequency of 5 mc/s, the transit time reduction factor in the shot noise formula is less than 0.01%, and can therefore be neglected.

The effective hole temperatures obtained are shown in figure 25, and are compared to those predicted in section 4.4. Equations (4.4.5) for $V < V_p$ and (4.4.9) for $V > V_p$ were used where the following parameters were substituted: $F_o = 1.5 \cdot 10^3$ volts/cm. (Ryder, 1953), $\mu_o = 1900$ cm^2/volt sec. (Conwell, 1958), $V_p = 6.0$ volts, and $W = 1.3 \cdot 10^{-3}$ cm.

The agreement between theoretical and experimental results is not very good, the experimental values for the average temperature lying below the theoretical ones for $V < V_p$, and above for $V > V_p$. A most likely source of error is in the value of the base width used, which was calculated from the manufacturer's data for f_α ; individual units may vary widely from this value. However, this could not explain the sudden jump of temperature that is observed at punch-through. This could only be caused by the appearance of a new noise generating mechanism, or a sudden shift in the emphasis given to various noise temperatures in the base. It is quite possible under the experimental conditions that either or both of excess noise and surface conduction were not absent, even though great care was taken to avoid them; in this respect it should be noted that one transistor showed an average noise temperature of 40,000 °K at punch-through, though in fact this figure could not truly represent the thermal noise temperature, but the noise due to

some other noise generating mechanism .

5.4   Conclusion

The d-c. and a-c. characteristics of the p-n-p diode have been measured and interpreted on the basis of present theories. The diode noise has been measured and where applicable interpreted in terms of noise temperatures; the latter are not found to agree with theory.

Further measurements that are recommended for obtaining more information are:

(a) noise and impedance measurements at frequencies higher than 5 mc/s, since it was not definitely established that excess noise was not present,

(b) measurements on p-n-p diodes with different punch-through voltages to obtain noise temperatures at different field strengths.

(c) measurements on n-p-n diodes to determine the noise temperatures of electrons, which are expected to be different from those of holes due to their different mobilities, and

(d) measurement of the cut-off frequency f_α of the transistors to obtain a more accurate value of the base width.

Appendix I

The Shockley Equations for a One-dimensional Ideal Transistor

Since in a p-n-p transistor the base width W is very much less than the diffusion length for holes in the base L_p, the transistor cannot be considered as two separate p-n junctions, but must be treated as a single unit. By considering bulk recombination and generation, and diffusion of holes, Shockley (1949) derived the following equations for the emitter and collector currents:

$$I_e = I_s\left[\left\{\coth\frac{W}{L}\right\}\left\{\exp\left(\frac{qV_e}{kT}\right)-1\right\} - \left\{\operatorname{csch}\frac{W}{L}\right\}\left\{\exp\left(\frac{qV_c}{kT}\right)-1\right\}\right] \qquad (A-1.1)$$

$$I_c = I_s\left[\left\{\coth\frac{W}{L}\right\}\left\{\exp\left(\frac{qV_c}{kT}\right)-1\right\} - \left\{\operatorname{csch}\frac{W}{L}\right\}\left\{\exp\left(\frac{qV_e}{kT}\right)-1\right\}\right] \qquad (A-1.2)$$

where
I_e = the current entering the emitter,
I_c = the current entering the collector,
V_e = the voltage of the emitter with respect to the base,
V_c = the voltage of the collector with respect to the

base, and I_s is the reverse saturation current of either junction given by equation (1.2.2).

When the transistor is operated as a diode with the base floating, $I_e = -I_c$ and the above equations yield

$$V_e = \frac{kT}{q}\ln\frac{2}{1-\exp\left(-\frac{qV}{kT}\right)} \qquad (A-1.3)$$

where the voltage across the diode $V = V_e - V_c$ has been substituted. The corresponding current is

$$I = I_e = -I_c = I_s\coth\frac{W}{2L}\tanh\frac{qV}{2kT} \qquad (A-1.4)$$

It should be noted here that the division of the voltage between V_e and V_c does not depend on $\frac{W}{L}$ whereas the current does. For $\frac{W}{L} \gg 1$, the current is given by

$$I = \frac{2q\,A\,P_n\,D}{W}\,\tanh\frac{qV}{2kT} \qquad (A\text{-}1.5)$$

where equation (1.2.2) has been substituted for I_s.

Appendix II

Combination of Shot Noise and Thermal Noise in a Solid

(a) The model we shall consider is that of an electron moving in a block of material with an externally applied voltage V; the field is uniform everywhere with a value $F = V/s$, where S is the length of the block. We shall assume that an electron undergoes collisions with the lattice with the probability of a collision per unit time being $1/\tau_0$; τ_0 is then the mean free time between collisions. Immediately after a collision an electron has on the average a velocity $\overline{u_1}$. Generation and recombination are assumed negligible, thus all carriers that enter one side leave the other. To find the spectral density of the current fluctuations we shall first find the autocorrelation function $\psi(\tau)$ for the component u of the electron velocity in the field direction; this is equal to the average value of the velocity at any time, times the velocity of the same electron at a time τ later. Thus $\psi_u(\tau) = \overline{u \cdot u(\tau)}$.

For a given initial velocity u, the average velocity at a time τ later will be given by

$$u(\tau) = \left[(\text{probability of no collision})(u + \frac{qF\tau}{m}) + (\text{probability of a collision})(\hat{u}(\tau)) \right] \left(\frac{t_0 - \tau}{t_0} \right)$$

where $\hat{u}(\tau)$ is the average velocity of an electron which has had at least one collision within the last τ of travel. The last multiplier takes into account the possibility of an electron leaving the specimen during τ, where t_0 is the transit time,

the average time taken by an electron to cross the specimen. Since we are interested in the noise from the specimen only we also have $\psi(\tau)=0$ for $\tau > t_0$.

For the statistics postulated above

$$u(\tau) = \left(\frac{t_0-\tau}{t_0}\right)\left\{\left(u-\overline{u}_1 - \frac{qF}{m}\tau_0\right)\exp\left(-\frac{\tau}{\tau_0}\right) + \overline{u}_1 + \frac{qF}{m}\tau_0\right\}.$$

To obtain the autocorrelation function this must be multiplied by u and averaged over all values of u; noting also that the mean velocity $\overline{u} = \overline{u}_1 + \frac{qF\tau_0}{m}$ we obtain

$$\psi_u(\tau) = \left(1 - \frac{\tau}{t_0}\right)\left\{\left(\overline{u^2} - \overline{u}^2\right)\exp\left(-\frac{\tau}{\tau_0}\right) + \overline{u}^2\right\}.$$

We now note that the current induced in the external circuit by an electron with velocity u is $\frac{qu}{s}$ and therefore

$$\psi_i(f) = \frac{q^2}{s^2}\psi_u(f).$$

The spectral density of the current fluctuations is obtained from integrating the autocorrelation function as follows,

$$S_i(f) = \frac{4nq^2}{s^2}\int_0^{t_0}\left(1 - \frac{\tau}{t_0}\right)\left\{\left(\overline{u^2} - \overline{u}^2\right)\exp\left(-\frac{\tau}{\tau_0}\right) + \overline{u}^2\right\}\cos\omega\tau\,d\tau$$

where n is the total number of electrons in the block, and $\omega = 2\pi f$. Making the assumption that $\tau_0 \ll t_0$, that is that an electron is subject to very many collisions during its transit, we now obtain

$$S_i(f) = \frac{4nq^2\tau_0}{s^2}\left(\overline{u^2} - \overline{u}^2\right)\left\{\frac{1}{1+\omega^2\tau_0^2}\right\} + \frac{4nq^2}{s^2}\frac{\overline{u}^2}{\omega^2\tau_0}\left(1 - \cos\omega t_0\right).$$

It is shown later, in (b), that the a-c. conductance is given by

$$G(f) = \frac{nq^2\tau_0}{ms^2}\left(\frac{1}{1+\omega^2\tau_0^2}\right)$$

and also noting that the mean current $I = \frac{nq\overline{u}}{s}$ and that the

transit time $t_0 = \frac{s}{\bar{u}}$, yields

$$S_i(f) = 4m\left(\overline{u^2} - \bar{u}^2\right) G(f) + 2qI\left\{\frac{\sin^2 \frac{1}{2}\omega t_0}{(\frac{1}{2}\omega t_0)^2}\right\}.$$

The second term of the last equation is the usual shot noise formula; the correction term at high frequencies is different from that of the vacuum diode since in the latter the electron undergoes constant acceleration while in the solid it has a constant drift velocity. The first term of the equation corresponds to the thermal noise and if we define the noise temperature by

$$T_n = \frac{m}{k}\left(\overline{u^2} - \bar{u}^2\right)$$

we have for frequencies much less than the reciprocal of the transit time

$$S_i(f) = 4kT_n G(f) + 2qI$$

The above definition of the noise temperature is convenient since it gives the noise in terms of the usual Nyquist formula, however it is the same temperature appropriate to a Maxwell velocity distribution with a mean velocity $\bar{u}$ and velocity variance $\overline{u^2} - \bar{u}^2$.

(b) The admittance of a specimen such as described above can be determined by examining the motion of a particular electron and determining its average velocity. Let us consider the field in the specimen to be of the form $F = F_0 + F_1 e^{j\omega t}$ then the velocity of an electron in the direction of the field at any time t will be given by

$$u(t) = u_1 + \int_T^t \frac{q}{m}\left(F_0 + F_1 e^{j\omega t'}\right) dt'$$

where u_1 is the velocity of the electron immediately after the last collision, which occurred at time T. Averaging over the various values of T and u_1 we obtain for the mean velocity of an electron at time t

$$\bar{u}(t) = \bar{u}_1 + \frac{q}{m}F_0\tau_0 + \frac{qF_1}{mj\omega}e^{j\omega t}\left(1 - \frac{1}{1+j\omega\tau_0}\right)$$

Introducing the external voltage $V = Fs$, the current in the external circuit $i = \frac{q\bar{u}}{s}$ for one electron, and the total number of electrons n, yields for the total current

$$I(t) = I_0 + I_1 e^{j\omega t}$$

$$I(t) = \frac{nq}{s}\cdot\left\{\bar{u}_1 + \frac{q}{ms}V_0\tau_0 + \frac{qV_1}{m\omega s j}e^{j\omega t}\left(1 - \frac{1}{1+j\omega\tau_0}\right)\right\}.$$

This immediately yields for the a-c. conductance

$$G(f) = \frac{nq^2\tau_0}{ms^2}\left\{\frac{1}{1+\omega^2\tau_0^2}\right\}.$$

The d-c. conductance is complicated by the nature of $\bar{u}_1$ which has a varying field dependence as discussed by Shockley (1951).

Literature Cited

Arthur J.B., Gibson A.F. and Granville J.W. (1956), Journal of Electronics 2 145, 259.

Brown W.L. (1953), Physical Review 91 518.

Conwell E. (1958), Proceedings of the I.R.E. 46 1281.

Dacey G.C. (1953), Physical Review 90 759.

Fröhlich H. and Paranjape B.V. (1956), Proceedings of the Physical Society B69 21, 866.

Götzberger A. (1959), Zeitschrift für Angewandte Physik 11 6.

Gunn J.B. (1957), Progress in Semiconductors 2 231.

Koenig (1958), Proceedings of the International Conference on Semiconductors, Rochester N.Y., Pergamon Press, p.227.

Larrabee R.D. (1959), Journal of Applied Physics 30 857.

Miller S.L. (1955), Physical Review 99 1234.

Nichol D.W. (1958), M.Sc. Thesis, University of British Columbia, Department of Physics.

Ryder E.J. (1953), Physical Review 90 766.

Schenkel H. and Statz H. (1954), Proceedings of the National Electronics Conference 10 614.

Shockley W. (1949), Bell System Technical Journal 28 435.

Shockley W. (1951), Bell System Technical Journal 30 990.

Shockley W. and Prim R.C. (1953), Physical Review 90 753.

Stratton R. (1958), Journal of Electronics and Control 5 157.

Thompson B.J., North D.O. and Harris W.A. (1940-41), R.C.A. Review, January 1940 to July 1941.

Yamashita J. and Watanabe M. (1954), Progress in Theoretical Physics 12 443.